2015 Fall

"Phase Transformation *in* Materials"

11.30.2015

Eun Soo Park

Office: 33-313
Telephone: 880-7221
Email: espark@snu.ac.kr
Office hours: by an appointment

Contents for previous class

< Phase Transformation in Solids >

1) Diffusional Transformation

(a) Precipitation

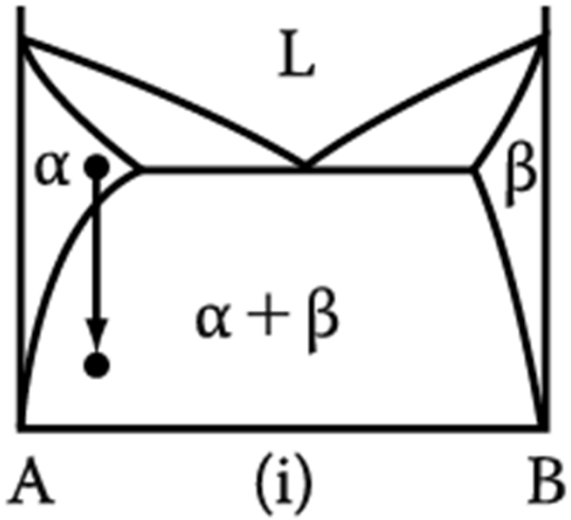

Homogeneous Nucleation

➡ Effect of misfit strain energy

$$\Delta G = -V\Delta G_V + A\gamma + V\Delta G_S$$

$$r^* = \frac{2\gamma}{(\Delta G_V - \Delta G_S)} \qquad \Delta G^* = \frac{16\pi\gamma^3}{3(\Delta G_V - \Delta G_S)^2}$$

$$N_{hom} = \omega C_0 \exp\left(-\frac{\Delta G_m}{kT}\right)\exp\left(-\frac{\Delta G^*}{kT}\right)$$

Heterogeneous Nucleation

➡ suitable nucleation sites ~ nonequilibrium defects

(creation of nucleus~destruction of a defect($-\Delta G_d$))

$$\Delta G_{het} = -V(\Delta G_V - \Delta G_S) + A\gamma - \Delta G_d$$

$$\frac{\Delta G^*_{het}}{\Delta G^*_{hom}} = \frac{V^*_{het}}{V^*_{hom}} = S(\theta)$$

$$\frac{N_{het}}{N_{hom}} = \frac{C_1}{C_0}\exp\left(\frac{\Delta G^*_{hom} - \Delta G^*_{het}}{kT}\right)$$

Rate of Homogeneous Nucleation Varies with undercooling below T_e for alloy X_0

Effective equilibrium temperature is reduced by misfit strain E term, ΔGs.

Thermodynamics

vs

Kinetics

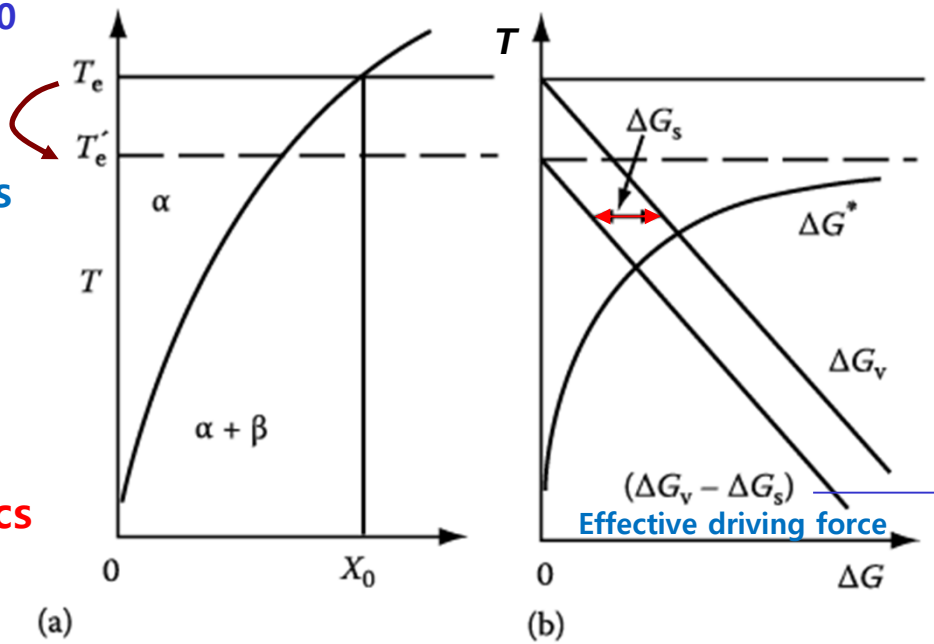

$$\Delta G_V \propto \Delta X \propto \Delta T$$

Composition dependent

$$\Delta G^* = \frac{16\pi\gamma^3}{3(\Delta G_V - \Delta G_S)^2}$$

Resultant energy barrier for nucleation

Critical undercooling ΔT_c

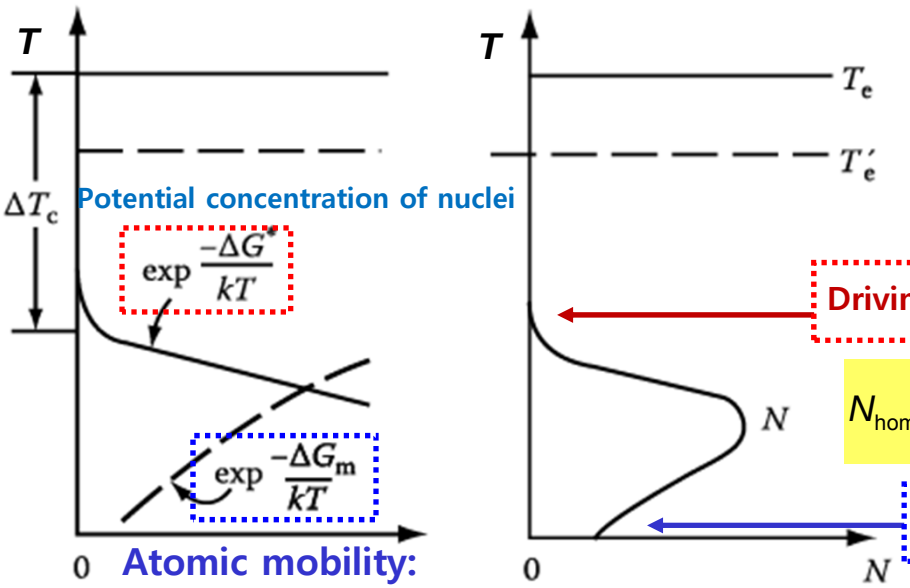

Driving force ΔG_v~too small → N~negligible

$$N_{hom} = \omega C_0 \exp\left(-\frac{\Delta G_m}{kT}\right)\exp\left(-\frac{\Delta G^*}{kT}\right)$$

Diffusion~too slow → N~negligible

Atomic mobility:

ΔG_m=const, T ↓ → ↓

ΔG_m : *activation energy for atomic migration*

Heterogeneous Nucleation in Solids

The Rate of Heterogeneous Nucleation during Precipitation

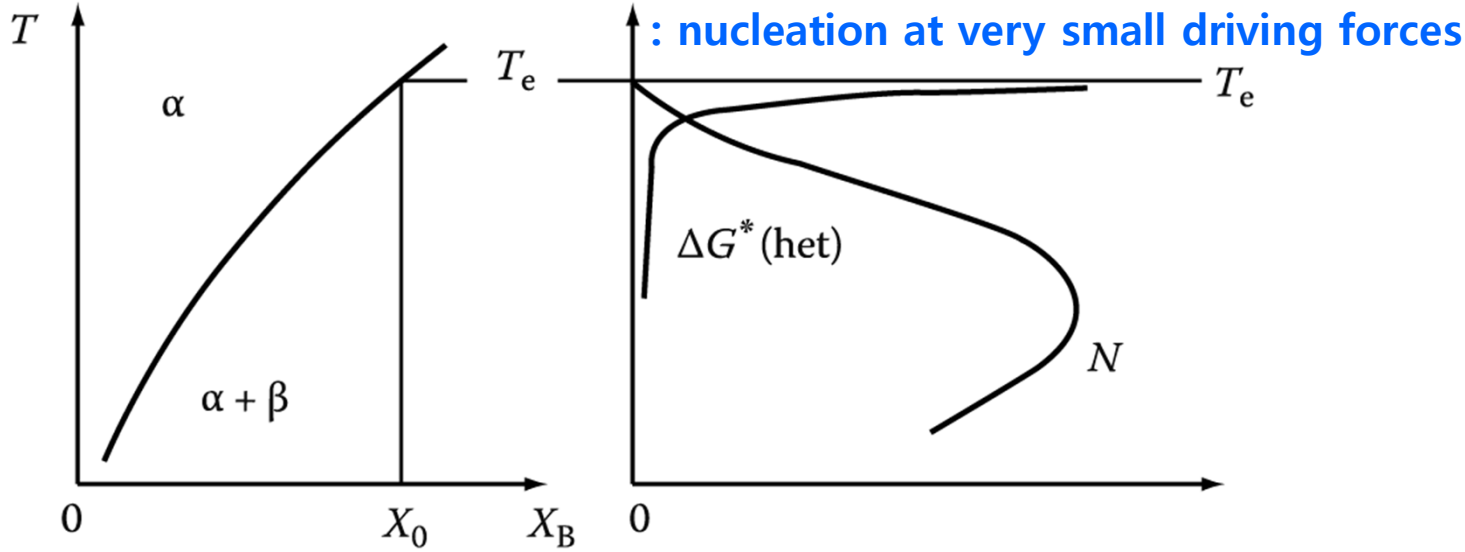

* Relative magnitudes of the heterogeneous and homogeneous volume nucleation rates

$$\frac{N_{het}}{N_{hom}} = \frac{C_1}{C_0}\exp\left(\frac{\Delta G^*_{hom} - \Delta G^*_{het}}{kT}\right)$$

Ignore ω and ΔG_m due to small deviation

ΔG* ~ always smallest for heterogeneous nucleation ⇨ **Exponential factor** : very large quantity ⇨ $\frac{N_{het}}{N_{hom}} > 1$ **High heterogeneous nucleation rate**

But, The factor C_1/C_0 ?

Heterogeneous Nucleation in Solids

$$\frac{N_{het}}{N_{hom}} = \frac{C_1}{C_0}\exp\left(\frac{\Delta G^*_{hom} - \Delta G^*_{het}}{kT}\right)$$

C_1/C_0 for Various Heterogeneous Nucleation Sites

각각의 핵생성처에서 경쟁적으로 핵생성 발생: 구동력 조건에 따라 전체 핵생성 속도에 dominant하게 영향을 미치는 site 변화

Grain boundary	Grain edge	Grain corner	Dislocations		Excess vacancies
$D = 50\ \mu m$	$D = 50\ \mu m$	$D = 50\ \mu m$	$10^5\ mm^{-2}$	$10^8\ mm^{-2}$	$X_v = 10^{-6}$
10^{-5}	10^{-10}	10^{-15}	10^{-8}	10^{-5}	10^{-6}

In order to make nucleation occur exclusively on the grain corner, how should the alloy be cooled?

1) At very small driving forces (ΔG_v), when activation energy barriers for nucleation are high, the highest nucleation rates will be produced by grain-corner nucleation.

핵생성 구동력
ΔG_v
↓
increase

2) dominant nucleation sites:
grain edges → grain boundaries

3) At very high driving forces it may be possible for the (C_1/C_0) term to dominate and then homogeneous nucleation provides the highest nucleation rates.

* The above comments concerned nucleation during isothermal transformations
(driving force for nucleation: [isothermal] constant ↔ [continuous cooling] increase with time)

- # Precipitate growth

1) Growth behind Planar Incoherent Interfaces

Diffusion-Controlled Thickening:

$$x \propto \sqrt{(Dt)}$$ Parabolic growth

$$v = \frac{D(\Delta C_0)^2}{2(C_\beta - C_e)(C_\beta - C_0)x}$$

$$v \propto \Delta X_0 \propto \sqrt{(D/t)}$$

Supersaturation

2) Diffusion Controlled lengthening of Plates or Needles

Diffusion Controlled lengthening:

$$v = \frac{D\Delta X_0}{k(X_\beta - X_r)} \cdot \frac{1}{r}\left(1 - \frac{r^*}{r}\right)$$

$v \rightarrow$ constant $\rightarrow$ $x \propto t$

Linear growth

3) Thickening of Plate-like Precipitates

Thickening of Plate-like Precipitates by Ledge Mechanism

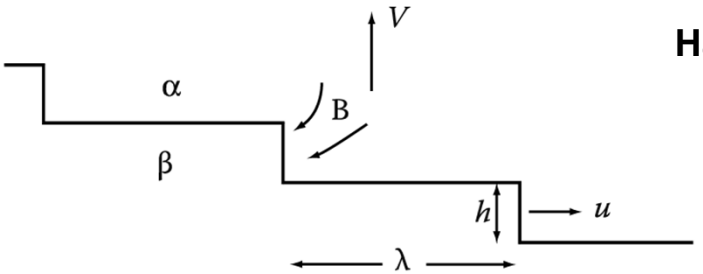

Half Thickness Increase

$$v = \frac{uh}{\lambda} \longrightarrow v = \frac{D\Delta X_0}{k(X_\beta - X_e)\lambda}$$

u : rate of lateral migration

5.4 Overall Transformation Kinetics

If isothermal transformation,

The fraction of Transformation as a function of Time and Temp. → f (t,T)

TTT Diagram ⟺ CCT Diagram

*** Constant Nucleation Rate Conditions**

$$f(t) = 1 - \exp\left(-f_e(t)\right) = 1 - \exp\left(-\frac{\pi}{3} I v^3 t^4\right)$$

*** Short time:**
1-exp(z)~Z (z ≪1)

*** Long time:**
t→∞, f →1

Johnson-Mehl-Avrami Equation

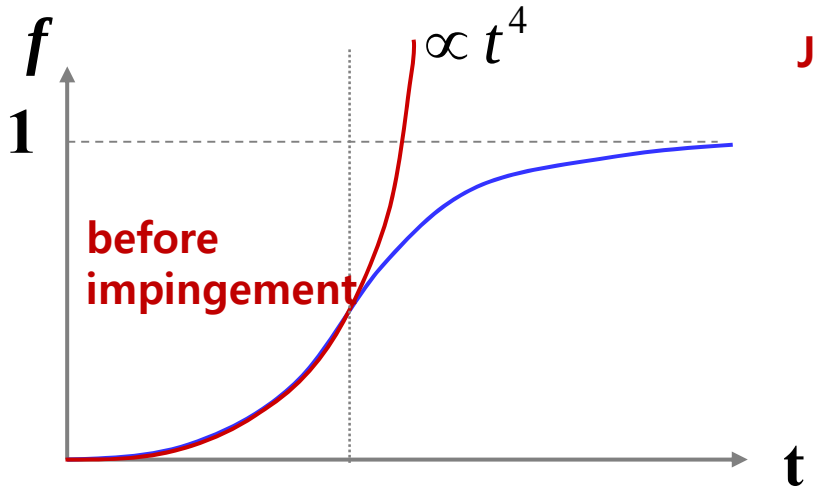

$$f = 1 - \exp\left(-kt^n\right)$$

***k*: *T* sensitive *f*(*I*, *v*)** $\quad -\frac{\pi}{3} I v^3$

***n*: 1 ~ 4 (depend on nucleation mecnanism)**

Growth controlled. **Nucleation-controlled.**

If no change of nucleation mechanism during phase transformation, n is not related to T.

i.e. 50% transform

Exp (-0.7) = 0.5

$$kt_{0.5}^n = 0.7 \qquad t_{0.5} = \frac{0.7}{k^{1/n}} \xrightarrow{\frac{\pi}{3} I v^3} t_{0.5} = \frac{0.9}{N^{1/4} v^{3/4}}$$

Rapid transformations are associated with (large values of k), or (rapid nucleation and growth rates)

Contents for today's class

- **Precipitation in Age-Hardening Alloys**
- **Quenched-in Vacancy**
- **Age hardening**
- **Spinodal Decomposition**

Q1: Precipitation in Age-Hardening Alloys

The theory of nucleation and growth can provide general guidelines for understanding civilian transformation.

5.5 Precipitation in Age-Hardening Alloys

Table 5.2 Some precipitation-Hardening Sequences

Base Metal	Alloy	Precipitation Sequence
Aluminum	Al–Ag	GPZ (spheres) $\rightarrow \gamma'$ (plates) $\rightarrow \gamma$ (Ag_2Al)
	Al–Cu	GPZ (disks) $\rightarrow \theta''$ (disks) $\rightarrow \theta'$ (plates) $\rightarrow \theta$ ($CuAl_2$)
	Al–Cu–Mg	GPZ (rods) $\rightarrow S'$ (laths) $\rightarrow S$ ($CuMgAl_2$) (laths)
	Al–Zn–Mg	GPZ (spheres) $\rightarrow \eta'$ (plates) $\rightarrow \eta$ ($MgZn_2$) (plates or rods)
	Al–Mg–Si	GPZ (rods) $\rightarrow \beta'$ (rods) $\rightarrow \beta$ (Mg_2Si) (plates)
Copper	Cu–Be	GPZ (disks) $\rightarrow \gamma' \rightarrow \gamma$ (CuBe)
	Cu–Co	GPZ (spheres) $\rightarrow \beta$ (Co) (plates)
Iron	Fe–C	ε-carbide (disks) $\rightarrow Fe_3C$ (plates)
	Fe–N	α'' (disks) $\rightarrow Fe_4N$
Nickel	Ni–Cr–Ti–Al	γ' (cubes or spheres)

Source: Mainly from Martin, J.W., in *Precipitation Hardening*, Pergamon Press, Oxford, 1968.

Let us now turn to a consideration of some examples of the great variety of civilian transformations in solid.

5.5 Precipitation in Age-Hardening Alloys

Precipitation in Aluminum-Copper Alloys

Al-4 wt%Cu (1.7 at %)

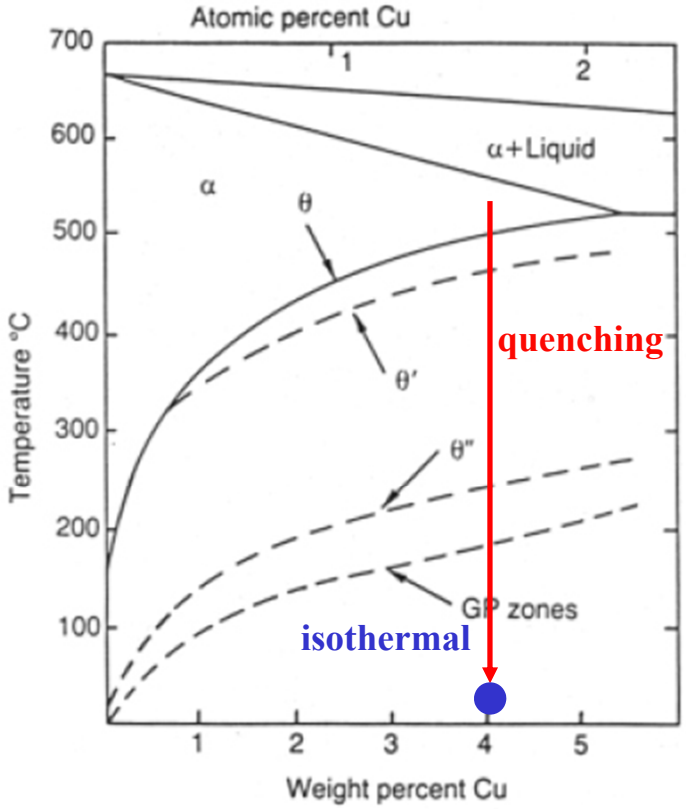

Fig. 5.25 Al-Cu phase diagram showing the metastable GP zone, Θ″ and Θ′ solvuses. (Reproduced from G. Lorimer, *Precipitation Processes in Solids*, K.C. Russell and H.I. Aaronson (Eds.), The Metallurgical Society of AMIE, 1978, p. 87.)

α_0 **540°C heat treatment → Quenching + Isothermal (below 180°C)**

Supersaturated solid solution

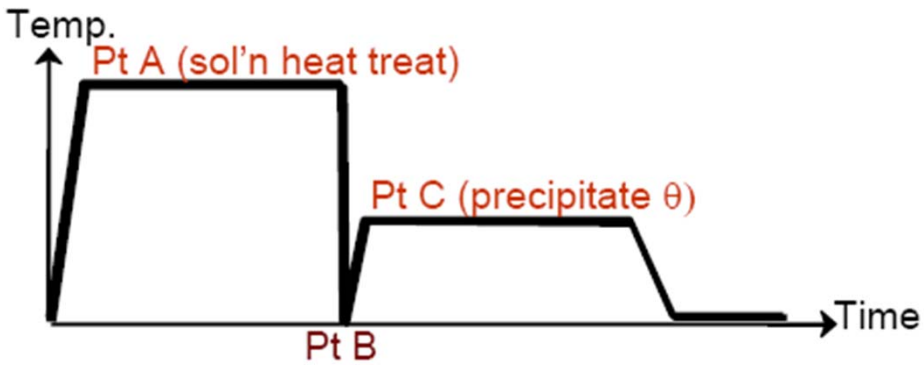

$\rightarrow \alpha_1$+GP zones

$\rightarrow \alpha_2 + \theta'' \rightarrow \alpha_3 + \theta' \rightarrow \alpha_4 + \theta$

$(CuAl_2)$

In most system, α, β phase~ different crystal structure → incoherent nuclei with large γ ~ impossible to homogeneous nucleation of β → Homogeneous nucleation of metastable phase β′ (GP Zones, Section 5.5.1)

Driving force for GP zone precipitation

5.5.1 GP Zones

$$\Delta G_{\theta}^{*} > (\Delta G_V - \Delta G_s) >> \Delta G_{zone}^{*}$$

The zones minimize their strain energy by choosing a disc-shape perpendicular to the elastically soft <100> directions in the fcc matrix (as shown in Fig. 5.26).

2 atomic layers thick and 10 nm in diameter with a spacing of ~10 nm

Fully coherent Cu-rich area with very low interfacial E

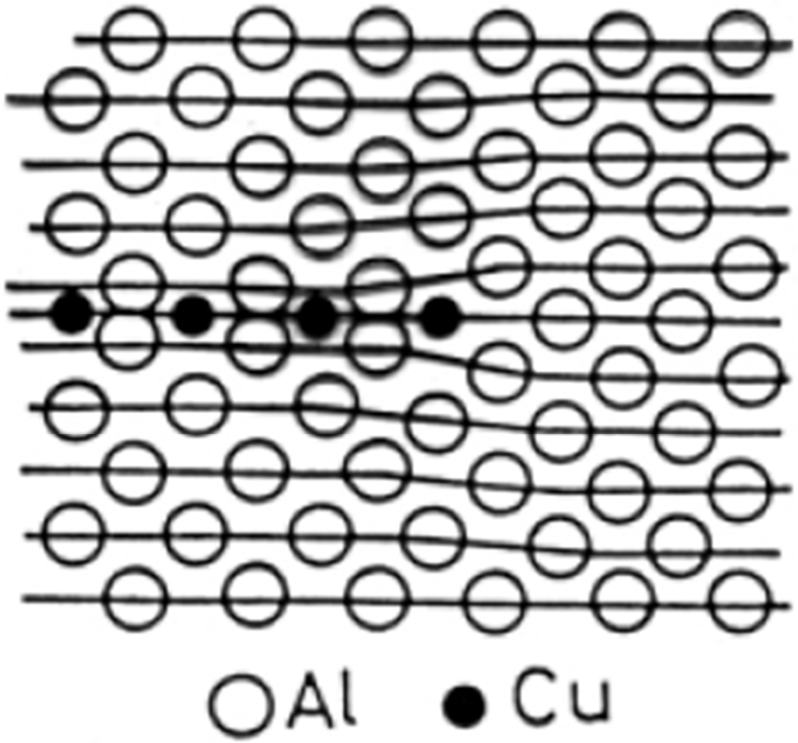

Fig. 5.26 Section through a GP zone parallel to the (200) plane. (Based on the work of V. Gerold: *Zeitschrift für Metallkunde* **45** (1954) 599.)

: 이러한 응집체는 완전한 석출 입자로 볼 수 없으며, 때때로 석출대 (zone)로 명명함.

The zone appear to be homogeneously nucleated, however, excess vacancies are thought to play an important role in their formation (be returned to later)

GP zones of Al-Cu alloys (x 720,000, TEM)

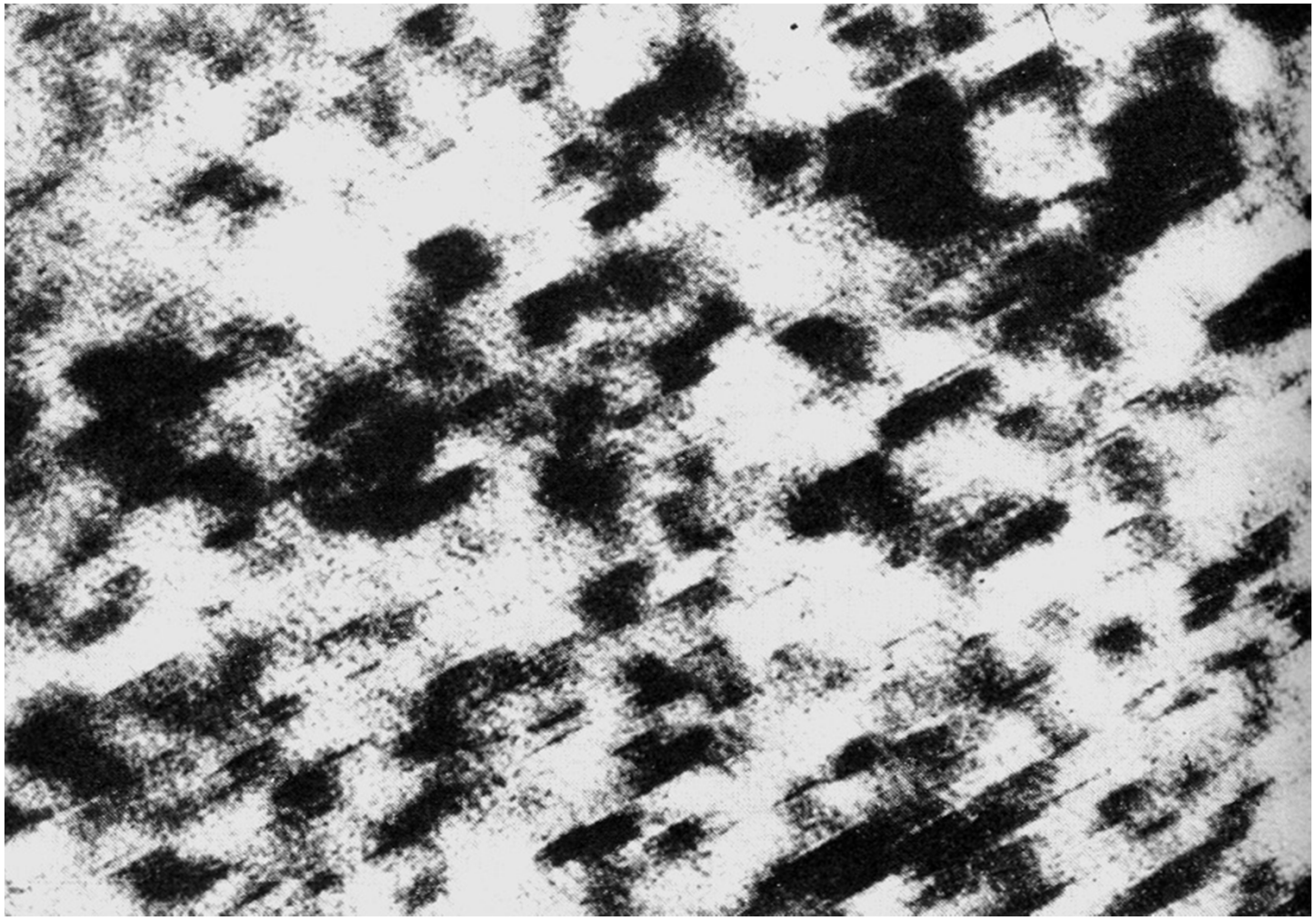

Fully coherent, about 2 atomic layers thick and
10 nm in diameter with a spacing of ~ 10 nm

: The contrast in the image is due to the coherency misfit strain perpendicular to the zones.
(Coherency misfit strain→local variations in the intensity of electron diffraction→image contrast change)

Transition phases

$\alpha_0 \rightarrow \alpha_1$+GP zone$\rightarrow \alpha_2$+$\theta''$ $\rightarrow \alpha_3$+θ' $\rightarrow \alpha_4$+θ ($CuAl_2$)

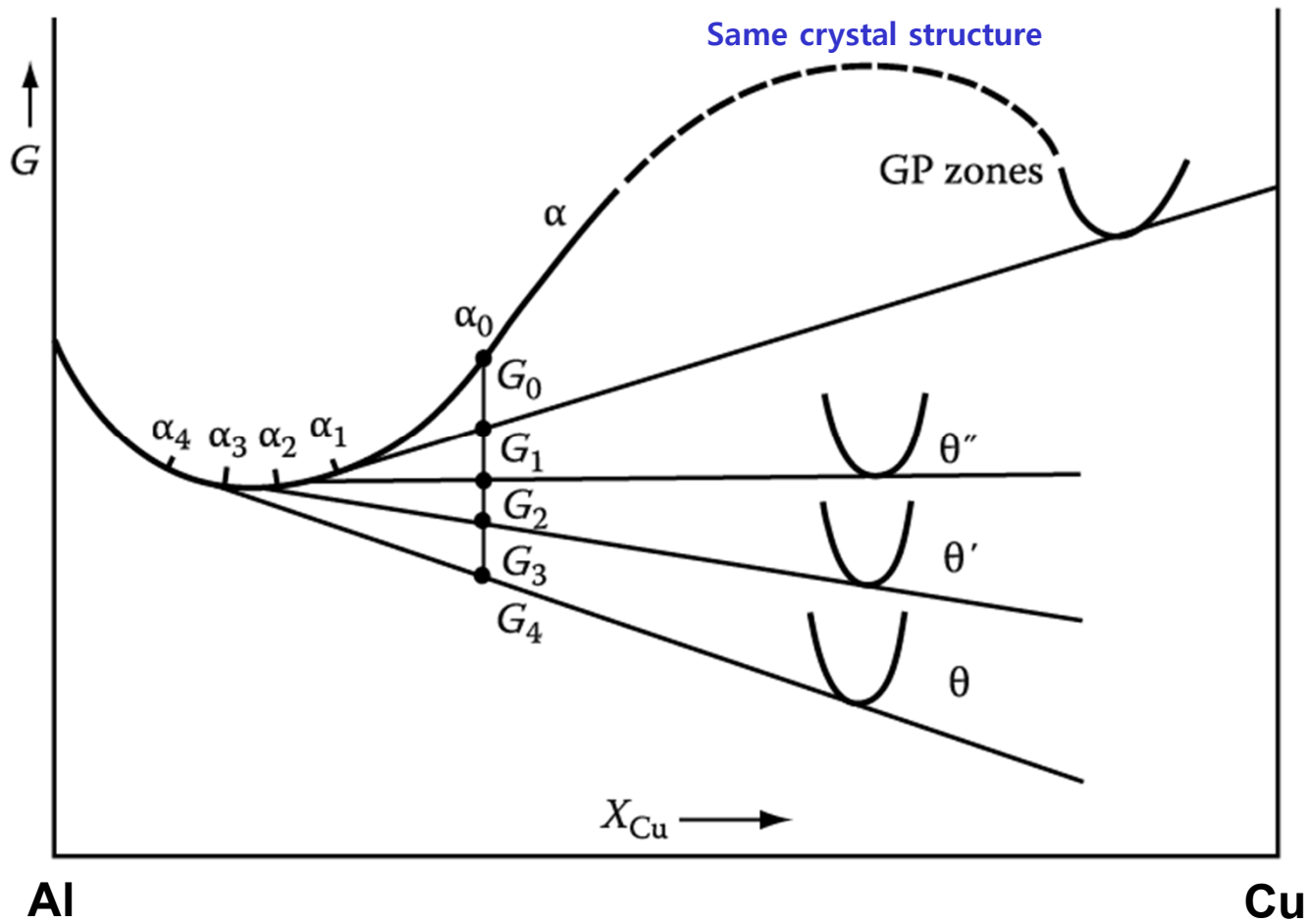

Fig. 5.27 A schematic molar free energy diagram for the Al-Cu system.

$\alpha_0 \rightarrow \alpha_1$+GP zone$\rightarrow\alpha_2+\theta'' \rightarrow\alpha_3+\theta' \rightarrow\alpha_4+\theta$ ($CuAl_2$)

Low Activation Energy of Transition Phases

➡ ∵ the crystal structures of the transition phases are intermediate between those of the matrix and the equilibrium phase.

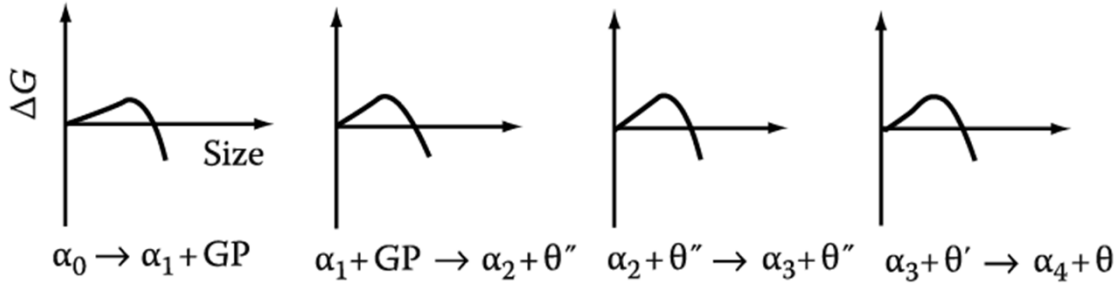

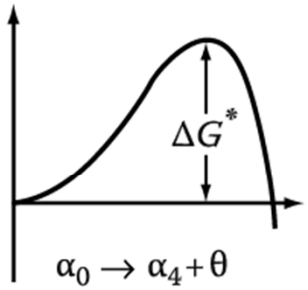

(a)

Transition phases (중간상, θ″ & θ′): a high degree of coherence, low interfacial E contribution to min ΔG*.

Equilibrium phase (평형상, θ): complex crystal structure that is incompatible with the matrix → high E interfaces and high ΔG*.

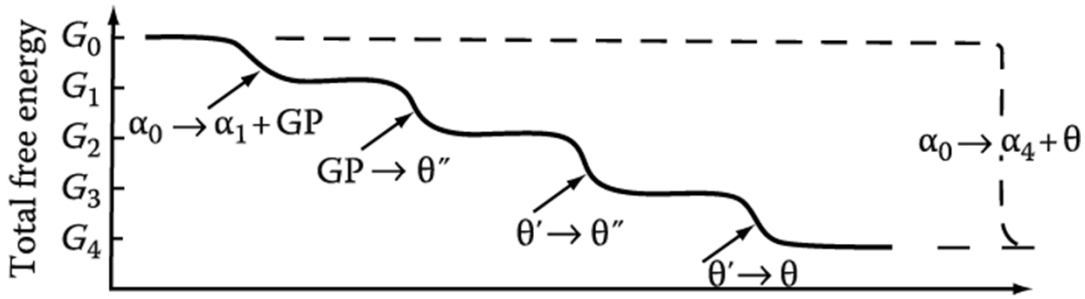

(b)

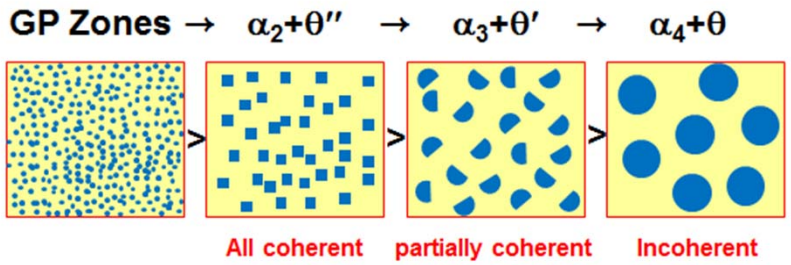

G of the alloy decreases more rapidly via the transition phases than by direct transformation to the equilibrium phase.

(a) The activation E barrier to the formation of each transition phase is very small in comparison to the barrier against the direct precipitation of the equilibrium phase. (b) Schematic diagram showing the total free E of the alloy versus time.

The Crystal Structures of θ″, θ′ and θ

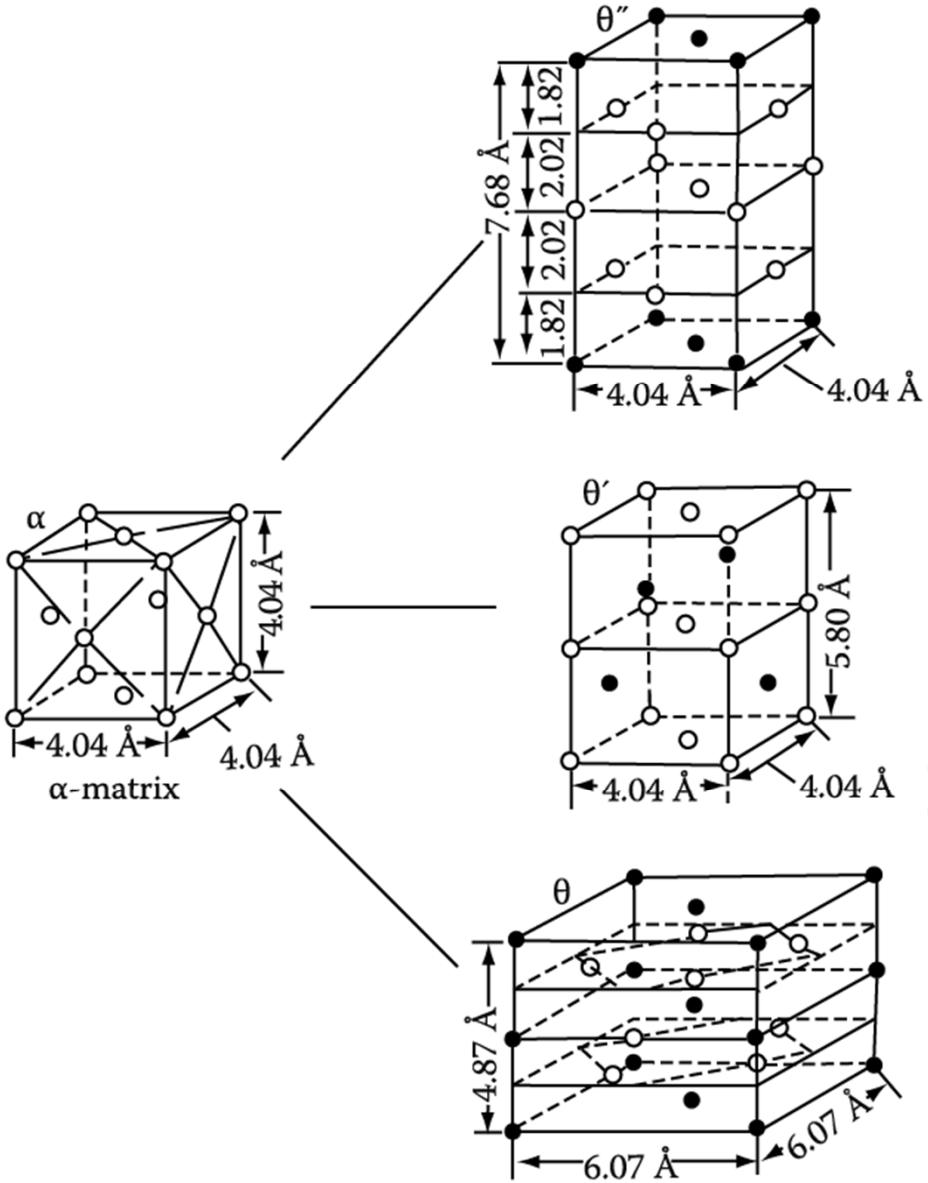

A tetragonal unit cell (= a distorted fcc structure in which the Cu and Al atoms are ordered on (001) planes.)

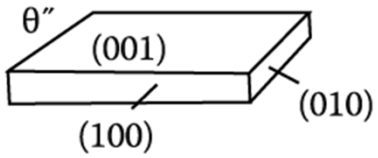

All sides coherent & a small distortion in the [001] direction of (010) and (100) faces

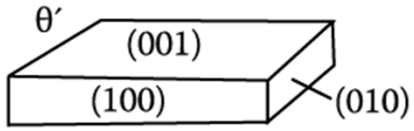

(001) Coherent or semicoherent

A tetragonal with an approximate composition $CuAl_2$

(100) (010) } Not coherent

Different crystal structure in (010) and (100) faces to the matrix and a large misfit in the [001] direction

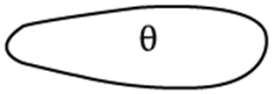

Incoherent

Approximate composition $CuAl_2$ and complex BCT structure

Fig. 5.29 Structure and morphology of θ'', θ' and θ in Al-Cu (○ Al. ● Cu).

θ″ of Al-Cu alloys (x 63,000, TEM)

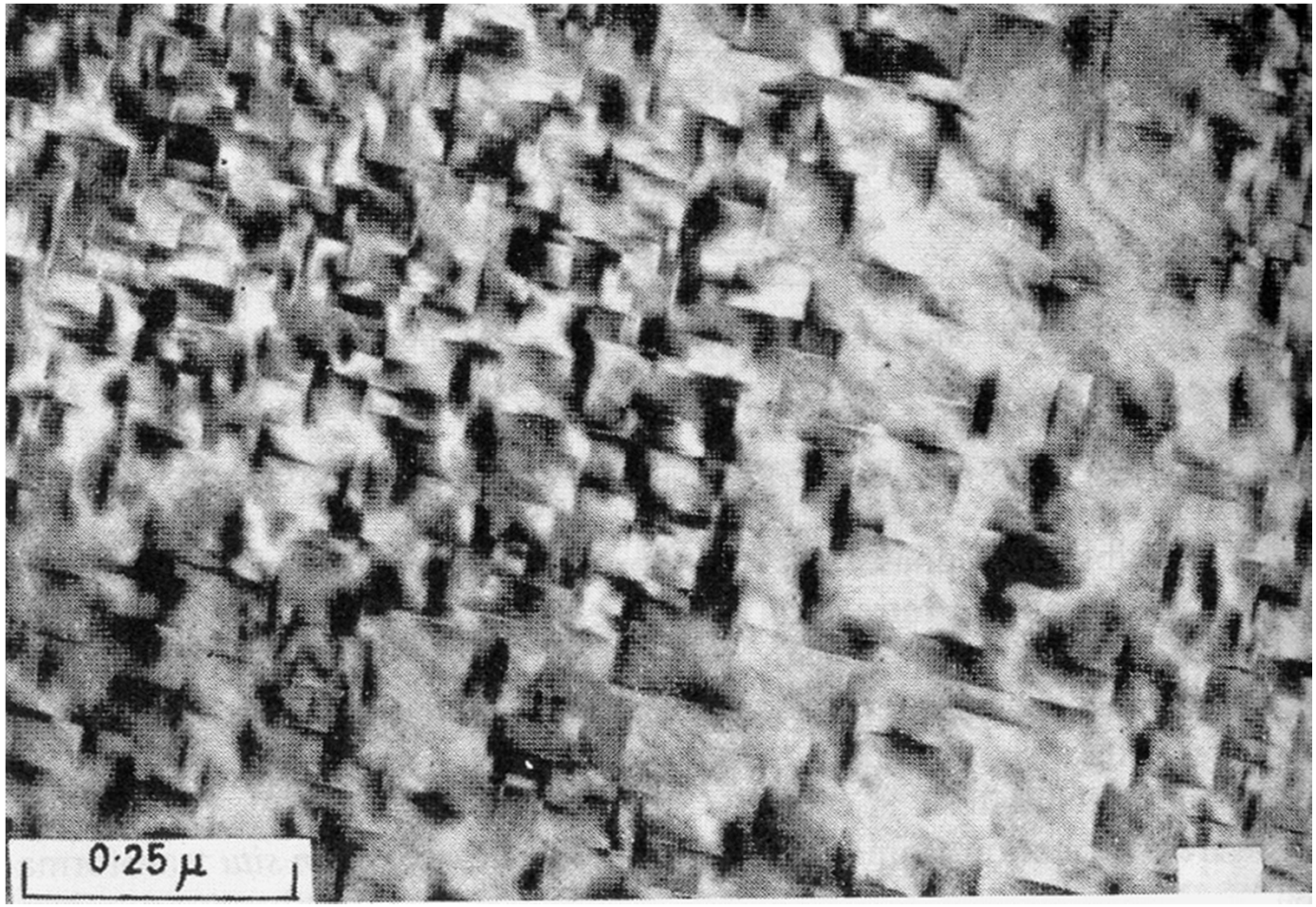

Tetragonal unit cell, essentially a distorted fcc in which Cu and Al atoms are ordered on (001) planes, fully-coherent plate-like ppt with $\{001\}_\alpha$ habit plane. ~ 10 nm thick and 100 nm in diameter (larger than GP zones).

: Like the GP zones, the θ″ precipitates are visible by virtue of the coherency-strain fields caused by the misfit perpendicular to the plates.

θ′ of Al-Cu alloys (x 18,000, TEM)

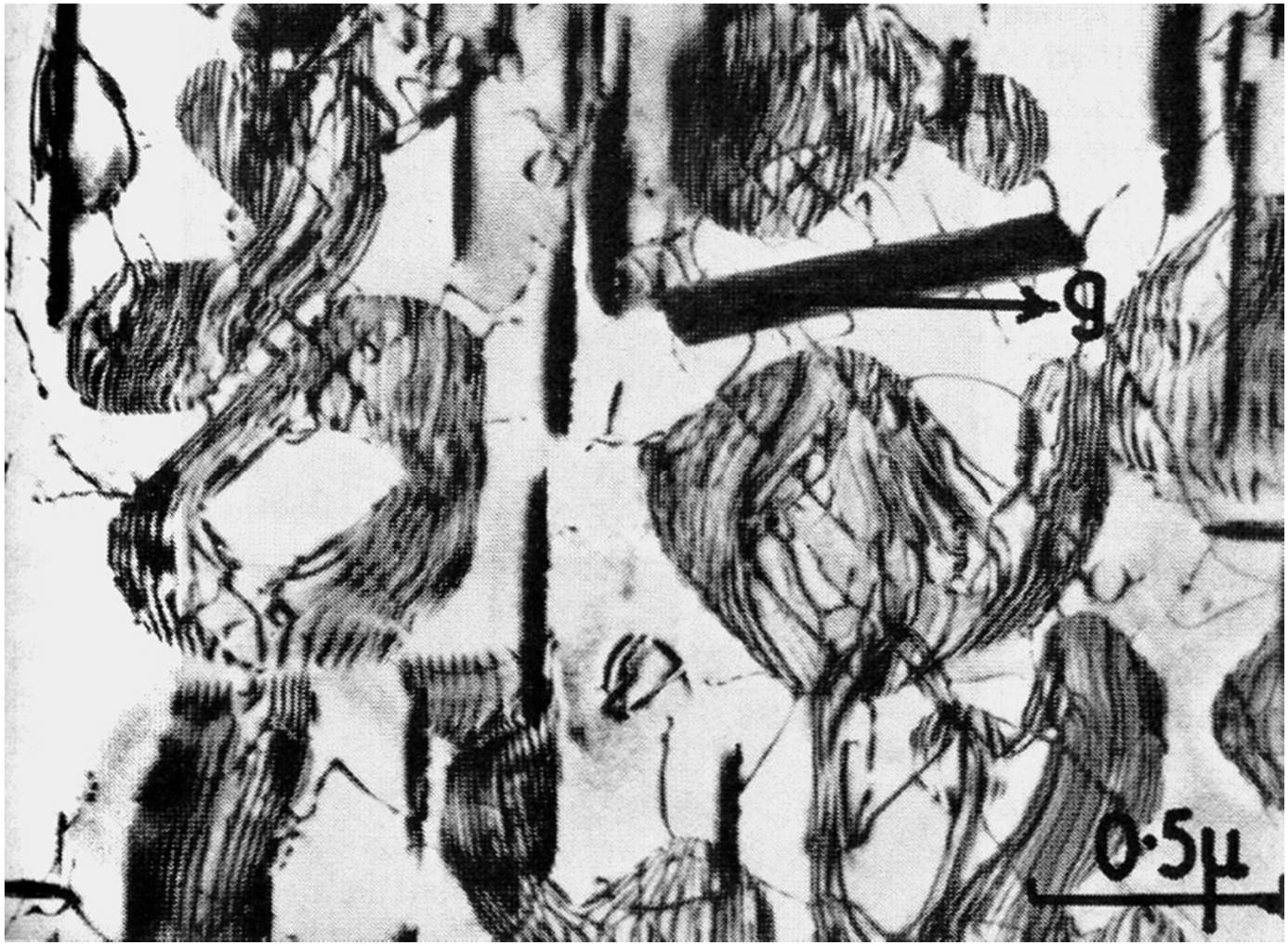

θ′ has (001) planes that are identical with $\{001\}_\alpha$ and forms as plates on $\{001\}_\alpha$ with the same orientation relationship as θ″. But, (100), (010) planes → incoherent, ~ 1 μm in diameter.

: The broad faces of the plates are initially fully coherent but lose coherency as the plates grow, while the edges of the plates are either incoherent or have a complex semicoherent structure.

θ of Al-Cu alloys x 8,000

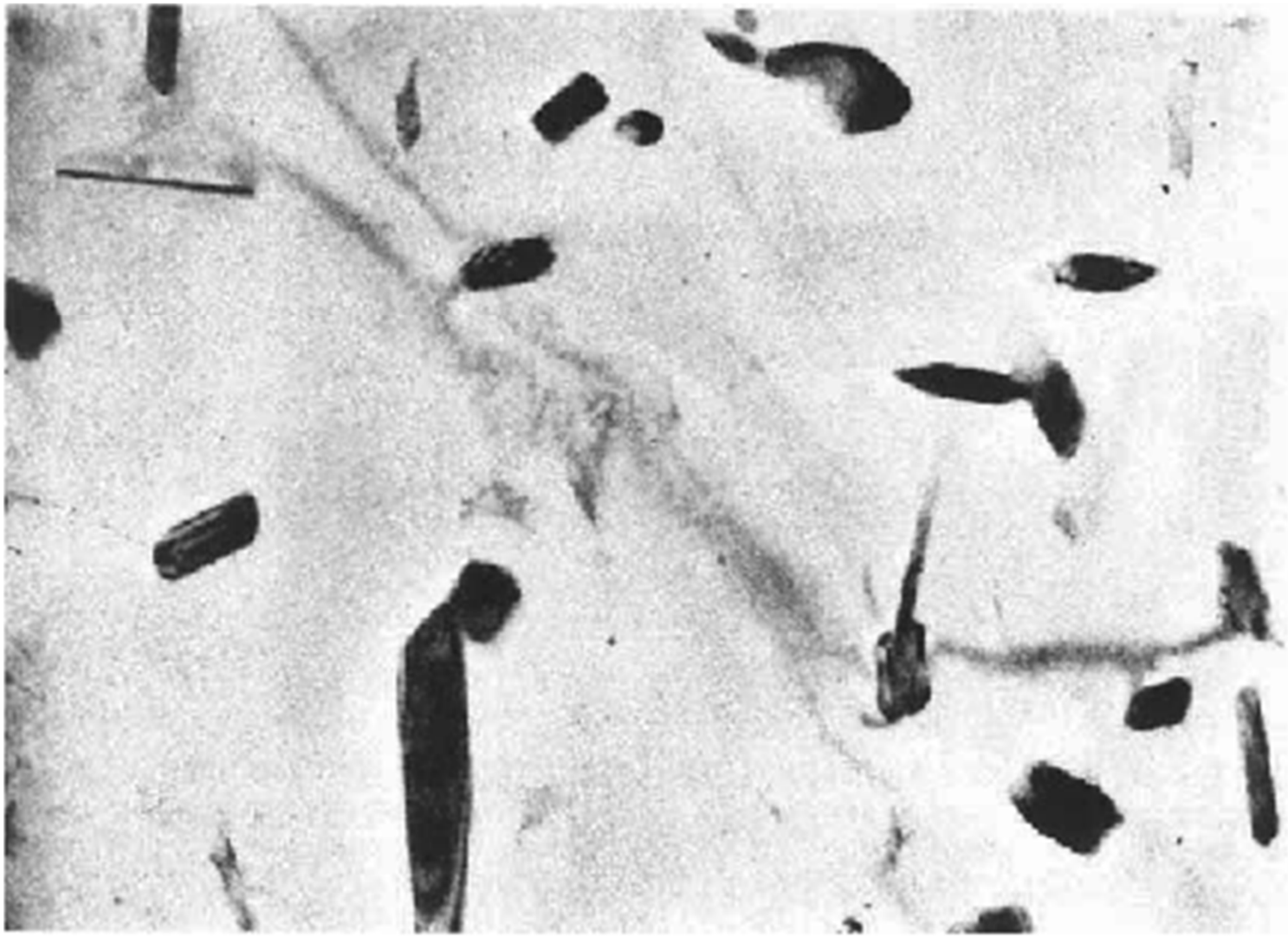

$CuAl_2$: complex body centered tetragonal, incoherent or complex semicoherent

: large size and coarse distribution of the precipitates

Nucleation sites

in Al-Cu alloys

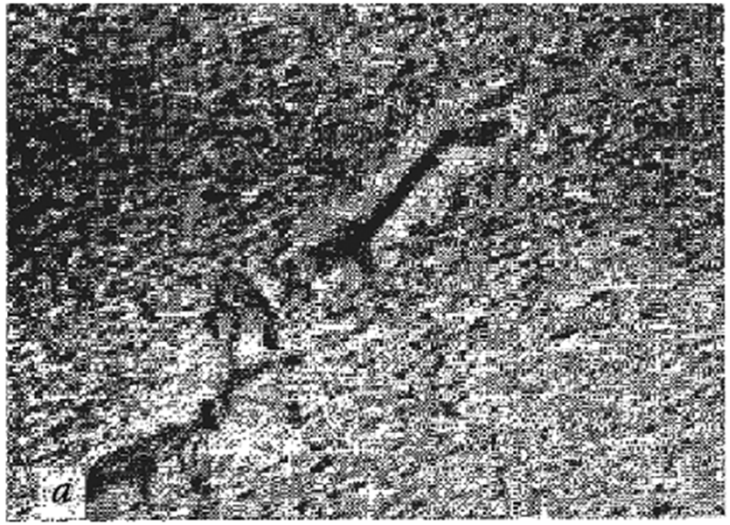

(a) θ” → θ’. θ’ nucleates at dislocation (x 70,000).

: Dislocation can reduce the misfit in two <100> matrix directions.

As the θ′ grows the surrounding, less-stable θ″ phase can be seen to dissolve.

(0) GP zones → θ”:

GP zones

~ very potent nucleation sites for θ”

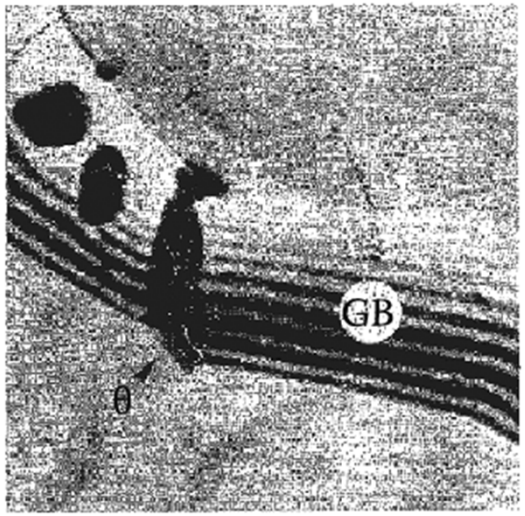

(b) θ nucleation on grain boundary (GB)(x 56,000)

: governed by the need to reduce the large interfacial energy contribution to ΔG* for this phase

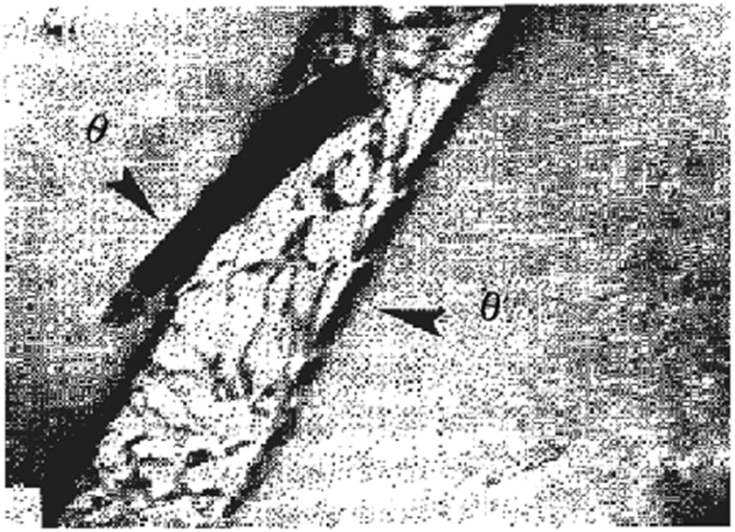

(c) θ’ → θ. θ nucleates at θ’/matrix interface (x 70,000).

Fig. 5.31 Electron micrographs showing nucleation sites in Al-Cu alloys.

* Effect of Aging Temperature on the Sequence of Precipitates

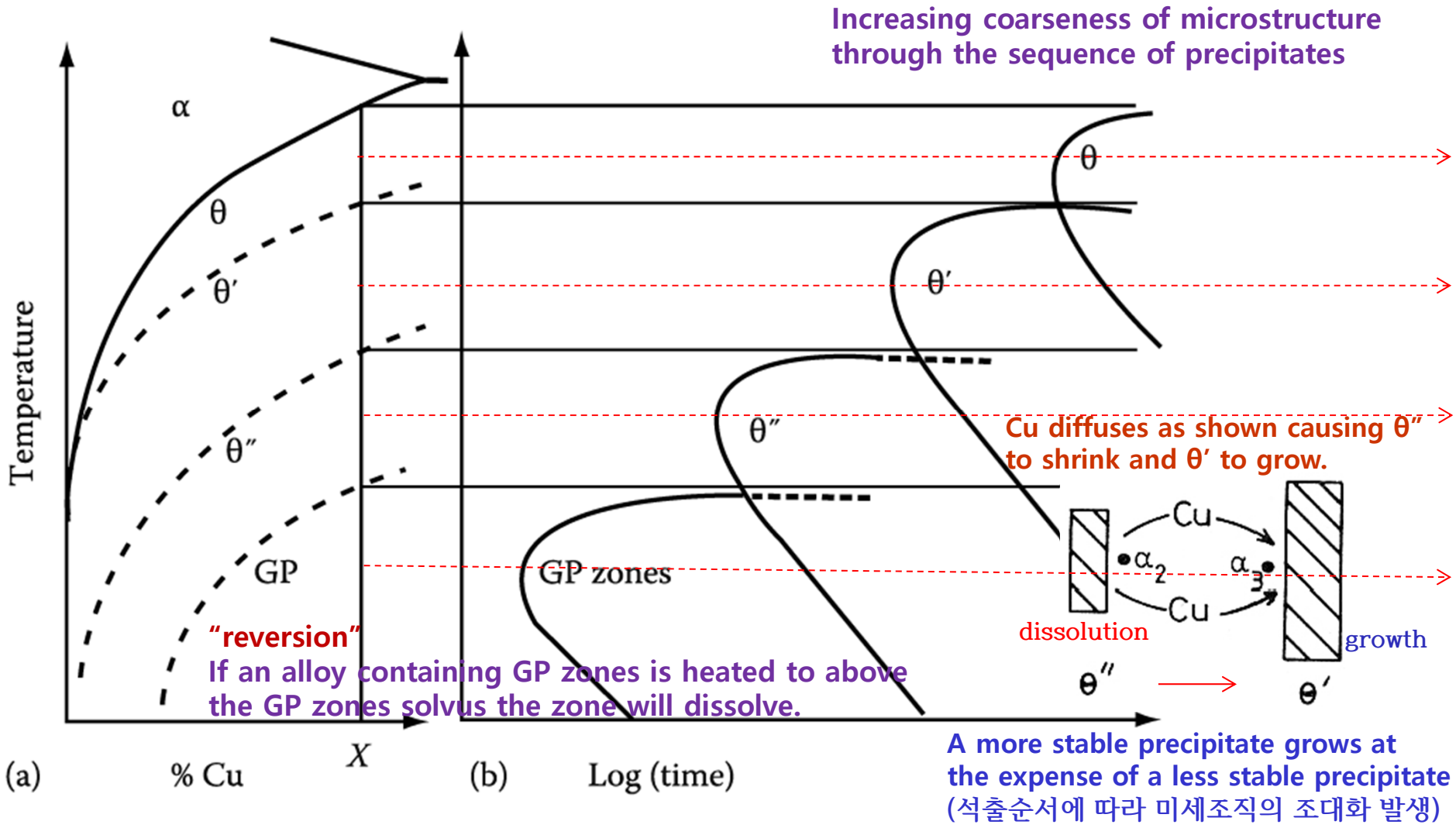

Fig. 5.32 (a) Metastable solvus lines in Al-Cu (schematic).
(b) Time for start of precipitation at different temperatures for alloy X in (a).

Q2: Quenched-in vacancies vs Precipitate-free zone

5.5.3. Quenched-in Vacancies

If $X_v < X_v^c$ critical vacancy supersaturation,
Precipitate nucleation X → formation of PFZ

In the vicinity of grain boundaries on subsequent aging,

a) Excess Ⓥ→ Ⓓ nucleation and moving ↑:
Heterogeneous nucleation sites ↑
b) Excess Ⓥ → atomic mobility ↑ at ageing temp:
speeds up the process of nucleation and growth
ex) rapid formation of GP zones at the relatively low aging temperature. (possible to RT aging in Al-Cu alloy)

a) Precipitate-Free Zone(PFZ) due to Vacancy Diffusion during quenching

Solute concentration within the zone ~ largely unchanged, but no precipitate at GB
∵ a critical vacancy supersaturation must be exceeded for nucleation to occur.

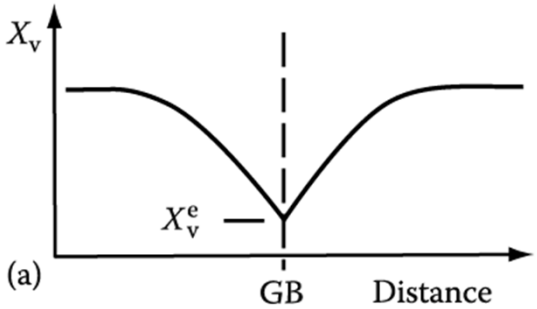

Similar PFZs can also form at inclusions and dislocations.

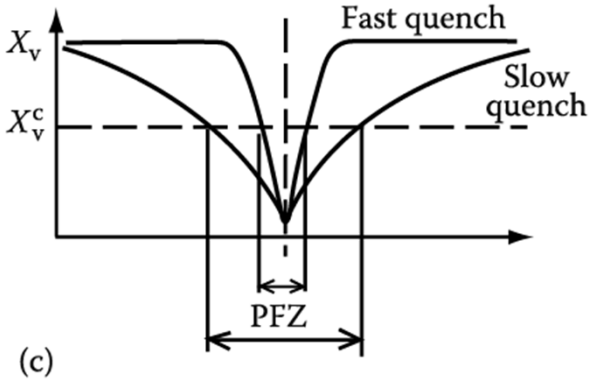

Fig. 5.35 A PFZ due to vacancy diffusion to a grain boundary during quenching.
(a) Vacancy concentration profile. (b) A PFZ in an Al-Ge alloy (x 20,000)
(c) Dependence of PFZ width on critical vacancy concentration X_v^c and rate of quenching.

* Equilibrium Vacancy Concentration

at equilibrium $\left(\frac{dG}{dX_V}\right)_{X_V = X_V^e} = 0$

$$\Delta H_V - T\Delta S_V + RT \ln X_V^e = 0$$

A constant ~3, independent of T

Rapidly increases with increasing T

$$X_V^e = \exp\frac{\Delta S_V}{R} \cdot \exp\frac{-\Delta H_V}{RT}$$

putting $\Delta G_V = \Delta H_V - T\Delta S_V$

$$X_V^e = \exp\frac{-\Delta G_V}{RT}$$

increases exponentially with increasing T

- **In practice, ΔH_V is of the order of 1 eV per atom and X_V^e reaches a value of about 10^{-4}~10^{-3} at the melting point of the solid**

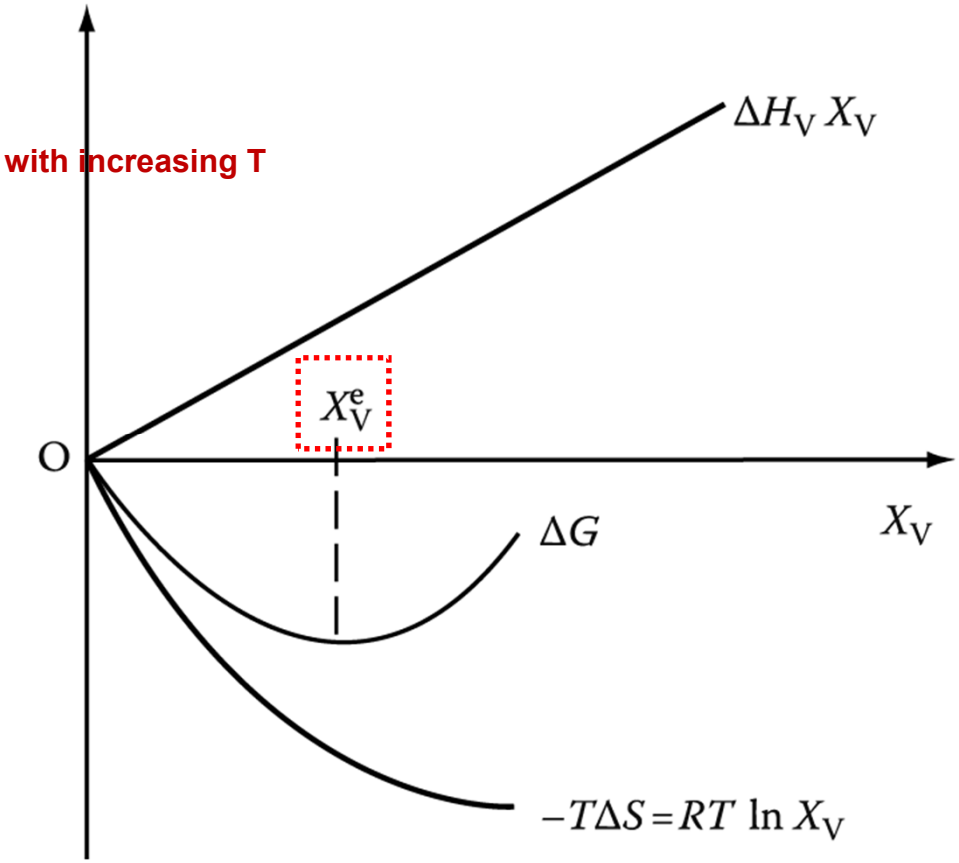

Fig. 1.37 Equilibrium vacancy concentration.

: adjust so as to reduce G to a minimum

b) Another cause of PFZs can be the nucleation and growth of GB precipitates during cooling from the solution treatment temperature.

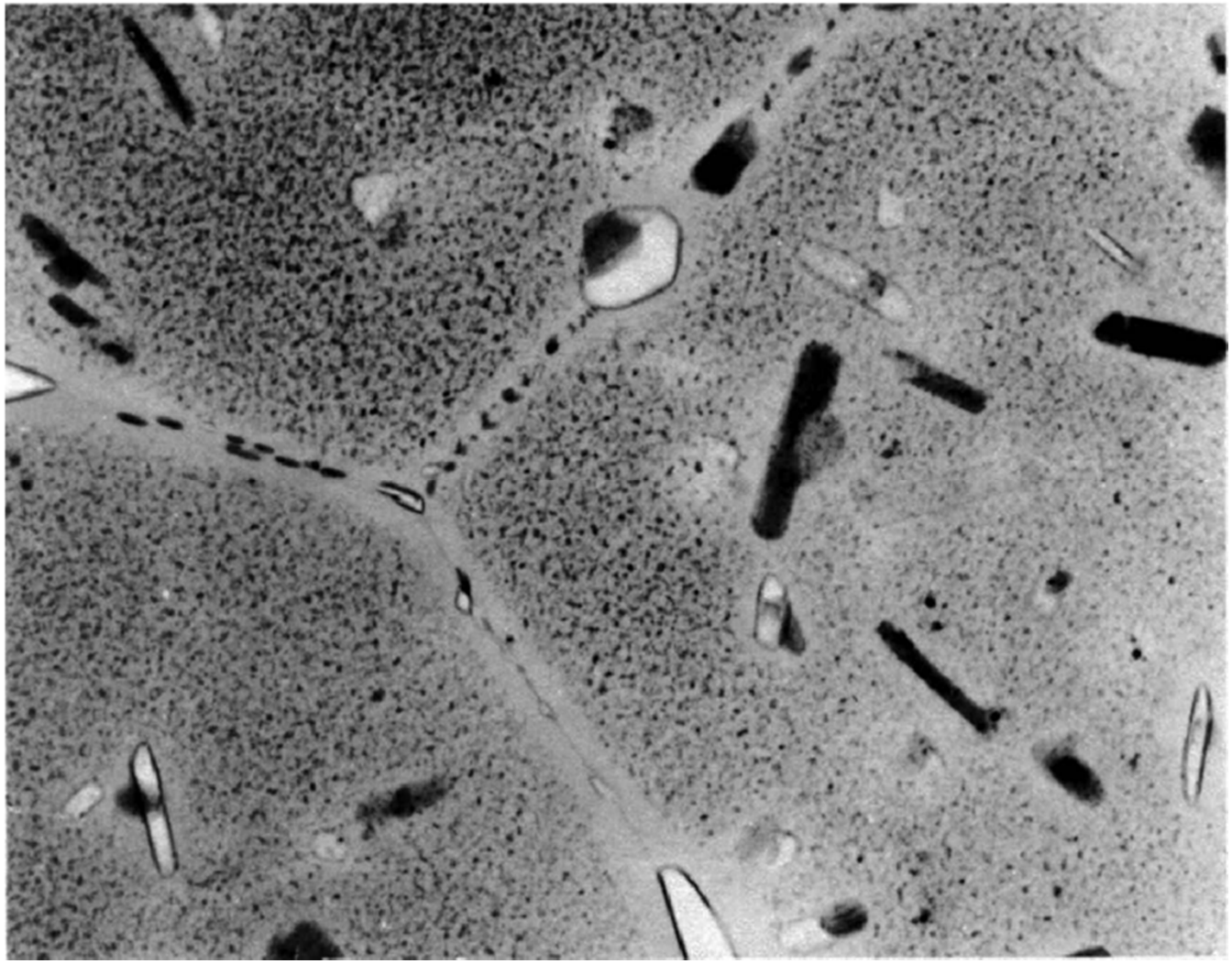

Fig. 5.36 PFZs around grain boundaries in a high-strength commercial Al-Zn-Mg-Cu alloy. Precipitates on grain boundaries have extracted solute from surrounding matrix. (x 59,200)

Q3: Age Hardening

5.5.4. Age Hardening

Transition phase precipitation → great improvement in the mechanical properties

Coherent precipitates→highly strained matrix→the main resistance to the Ⓓ movement: solid solution hardening

Hardness vs. Time by Ageing

Maximum hardness~ largest fraction of θ″
(coherent precipitates)

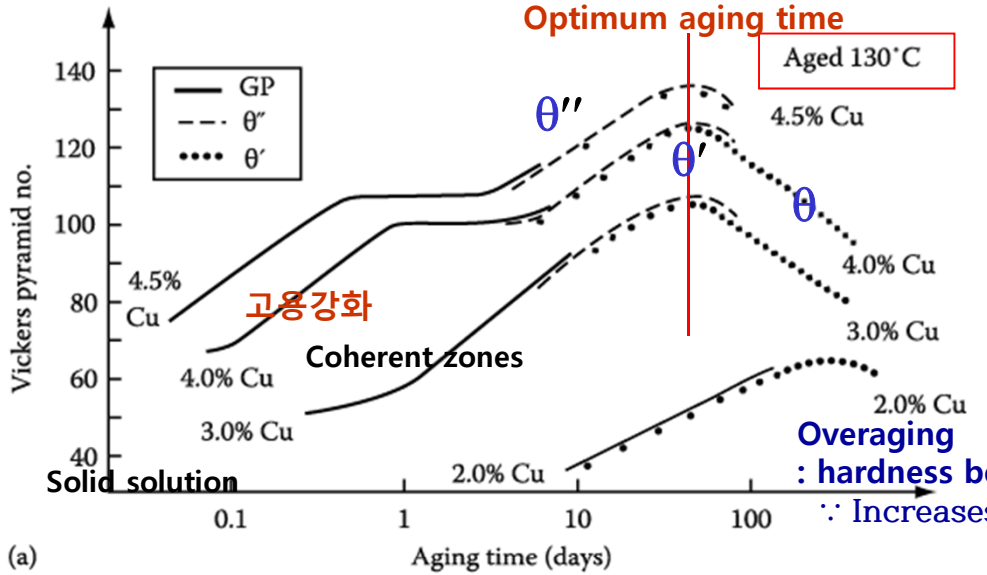

Ageing at 130°C produces higher maximum hardness than ageing at 190°C.

At 130°C, however, it takes too a long time (several tens of days).

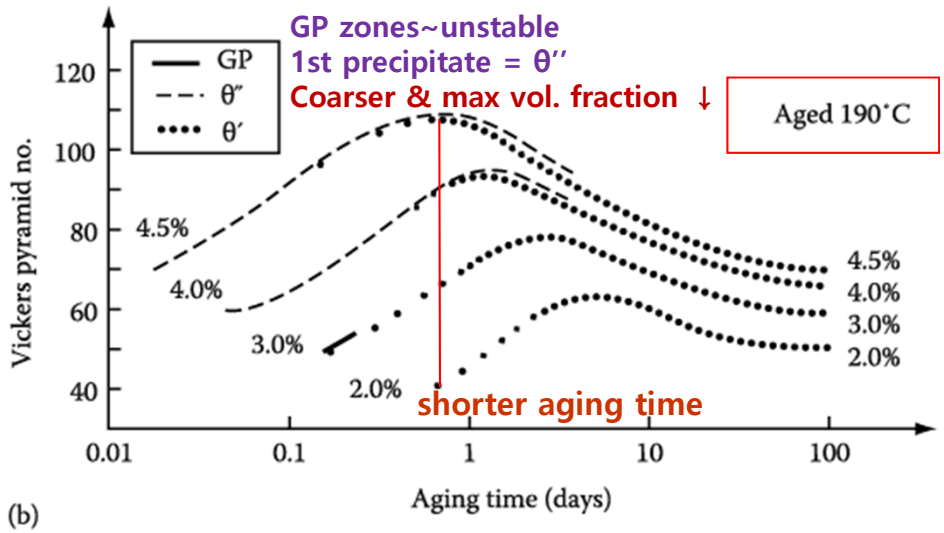

How can you get the high hardness for the relatively short ageing time (up to 24h)?

Double ageing treatment

first below the GP zone solvus → fine dispersion of GP zones then ageing at higher T.

: Engineering alloys are not heat treated for max. strength alone. → **to optimize other properties**
best heat treatment in practice

Fig. 5. 37 Hardness vs. time for various Al-Cu alloys at (a) 130 ℃ (b) 190 ℃

Q4: Spinodal Decomposition

5.5.5 Spinodal Decomposition

Spinodal mode of transformation has no barrier to nucleation

: describing the transformation of a system of two or more components in a metastable phase into two stable phases

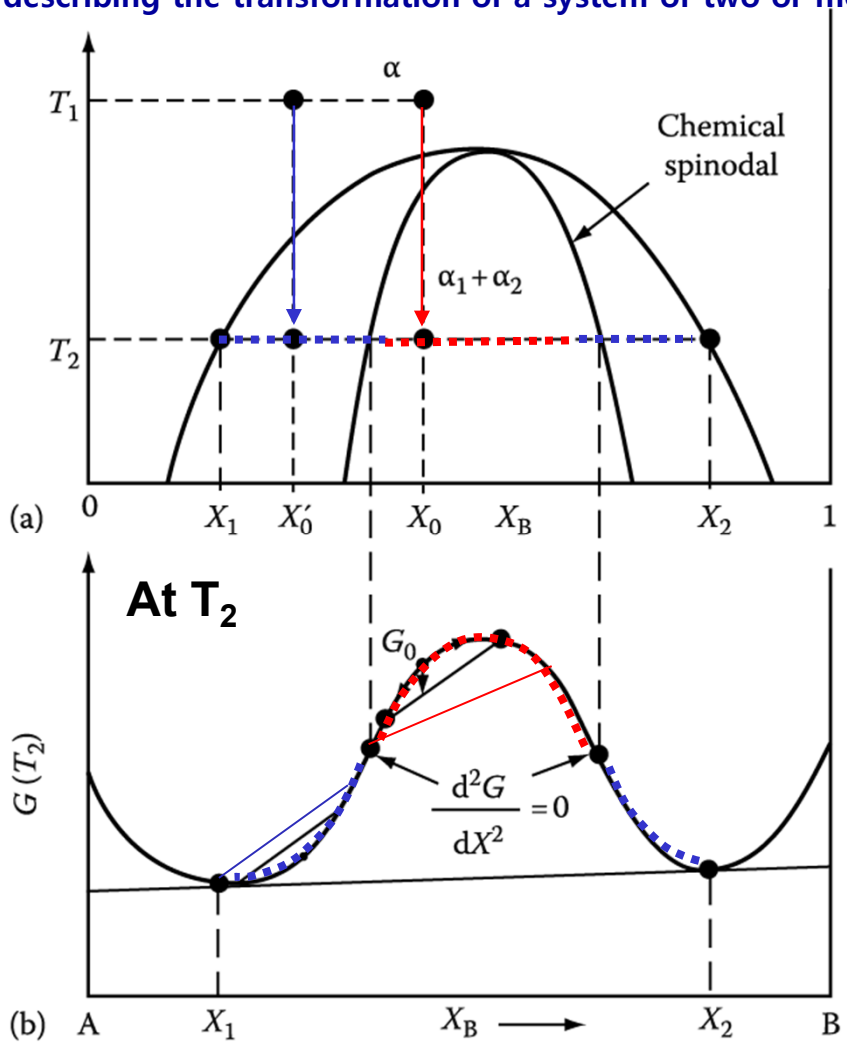

Fig. 5.38 Alloys between the spinodal points are unstable and can decompose into two coherent phasees α_1 and α_2 without overcoming an activation energy barrier. Alloys between the coherent miscibility gaps and the spinodal are metastable and can decompose only after nucleation of the other phase.

How does it differ between inside and outside the inflection point of Gibbs free energy curve?

1) Within the spinodal $\frac{d^2G}{dX^2}<0$

: phase separation by small fluctuations in composition/ "up-hill diffusion"

2) If the alloy lies outside the spinodal, small variation in composition leads to an increase in free energy and the alloy is therefore metastable.

The free energy can only be decreased if nuclei are formed with a composition very different from the matrix.

→ **nucleation and growth**

: "down-hill diffusion"

a) Composition fluctuations within the spinodal

b) Normal down-hill diffusion outside the spinodal

up-hill diffusion

down-hill diffusion

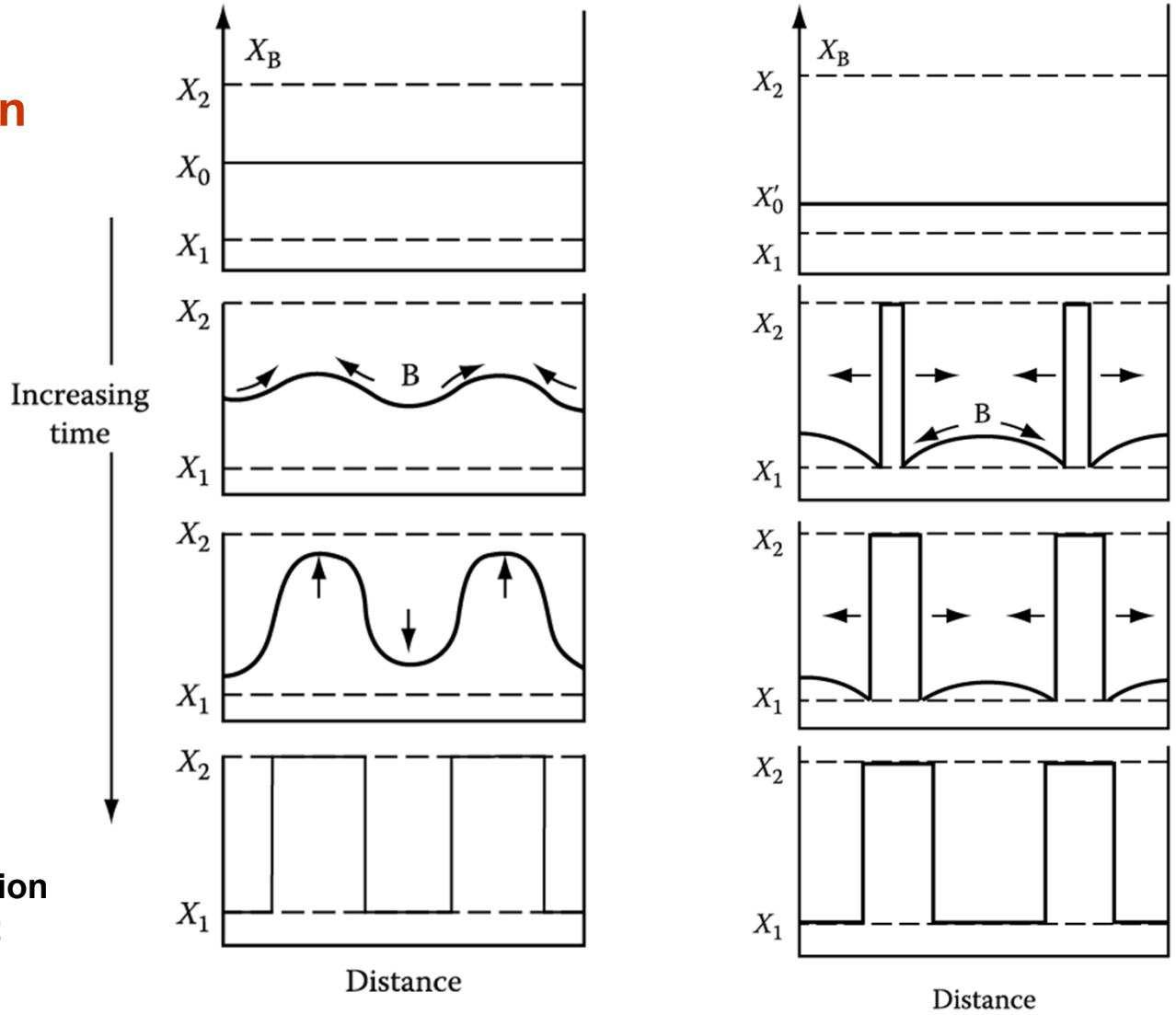

interdiffusion coefficient D<0

Fig. 5.39 & 5.40 schematic composition profiles at increasing times in (a) an alloy quenched into the spinodal region (X_0 in Figure 5.38) and (b) an alloy outside the spinodal points (X_0' in Figure 5.38)

Phase separation

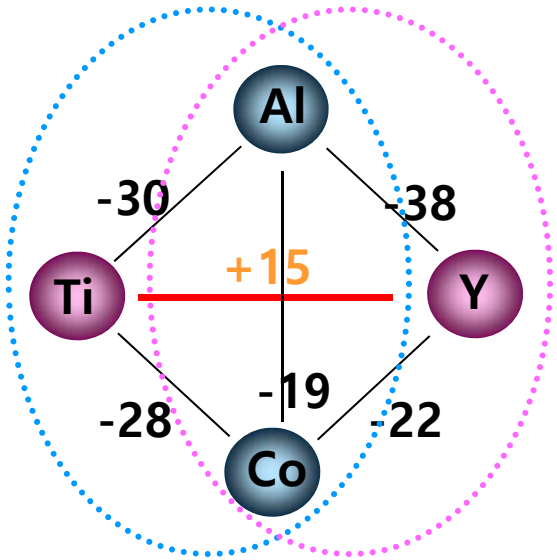

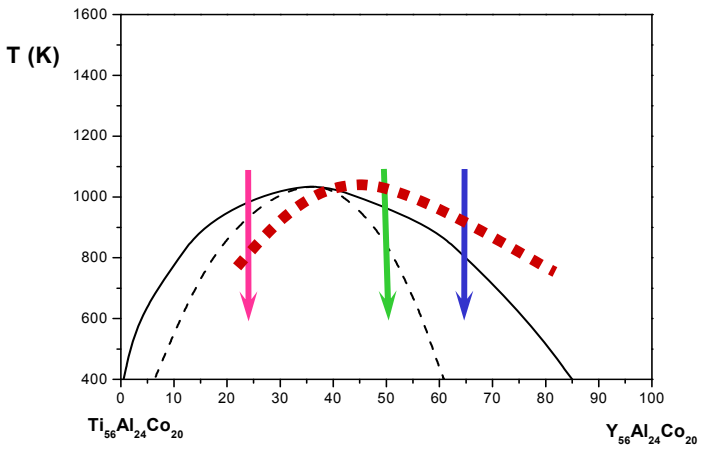

Droplet structure

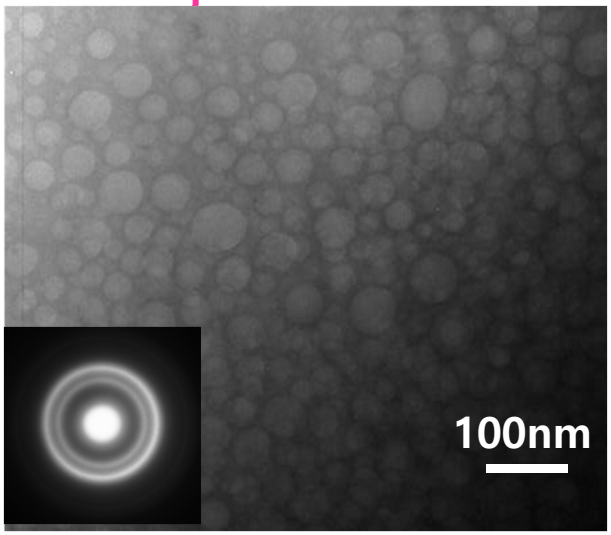

$(Y_{56}Al_{24}Co_{20})_{25}(Ti_{56}Al_{24}Co_{20})_{75}$

Interconnected structure

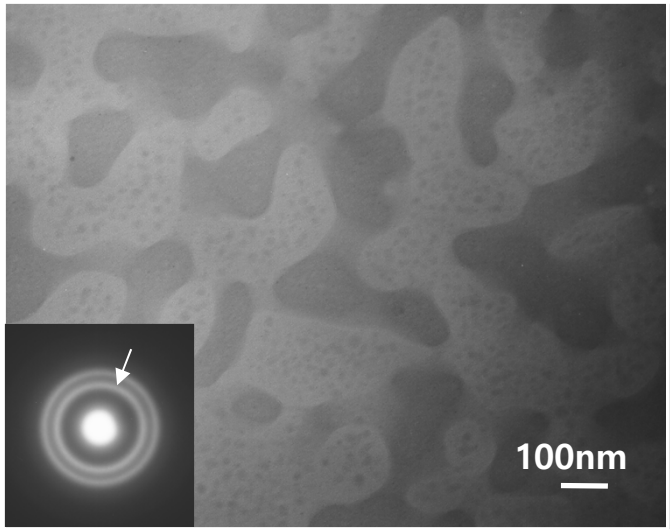

$(Y_{56}Al_{24}Co_{20})_{50}(Ti_{56}Al_{24}Co_{20})_{50}$

Droplet structure

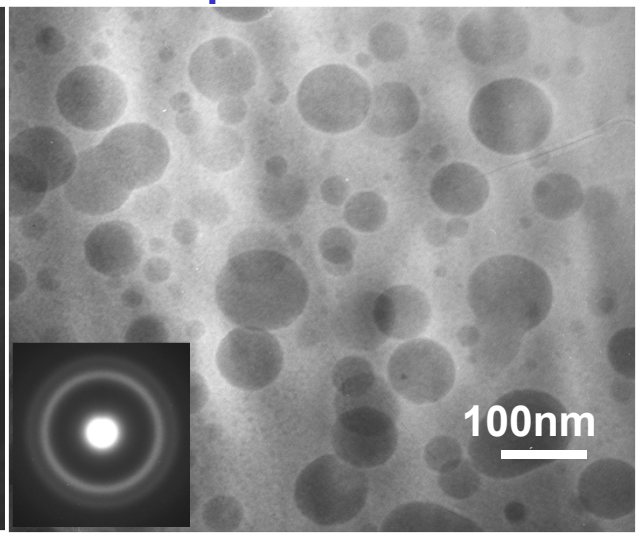

$(Y_{56}Al_{24}Co_{20})_{65}(Ti_{56}Al_{24}Co_{20})_{35}$

5.5.5 Spinodal Decomposition

* The Rate of Spinodal decomposition

a) Rate controlled by interdiffusion coefficient D (상호확산계수)

Within the spinodal D < 0,

composition fluctuation $\propto \exp(-t/\tau)$
(next page)

$$\tau = -\lambda^2 / 4\pi^2 D$$

τ: characteristic time constant
λ: wavelength of the composition modulations
(assumed one-dimensional)

b) Kinetics depends on λ: Transformation rate ↑ as λ ↓ (as small as possible).

But, minimum value of λ below which spinodal decomposition cannot occur.

Solutions to the diffusion equations

Ex1. Homogenization of sinusoidal varying composition in the elimination of segregation in casting

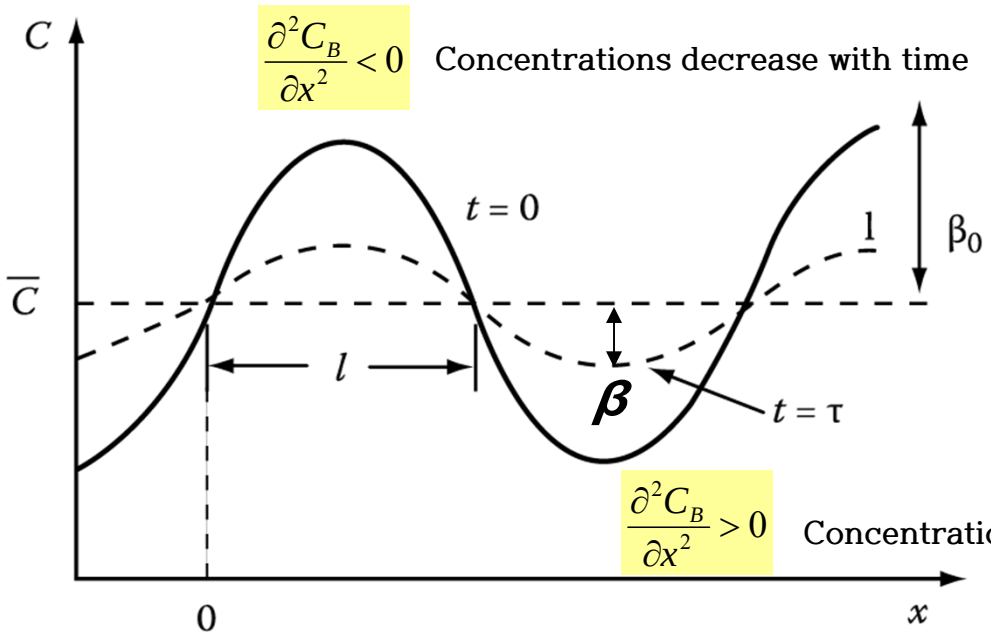

Fig. 2.10 The effect of diffusion on a sinusoidal variation of composition.

$$C = \overline{C} + \beta_0 \sin\frac{\pi x}{l} \quad \text{at t=0}$$

$$C = \overline{C} + \beta_0 \sin\frac{\pi x}{l} \exp\left(\frac{-t}{\tau}\right)$$

$$\beta = \beta_0 \exp(-t/\tau) \quad at \quad x = \frac{l}{2}$$

Amplitude of the concentration profile (β) decreases exponentially with time, $C \Rightarrow \overline{C}$

$$\tau = \frac{l^2}{\pi^2 D}$$

τ : relaxation time

"decide homogenization rate"

The initial concentration profile will not usually be sinusoidal, but in general any concentration profile can be considered as the sum of an infinite series of sine waves of varying wavelength and amplitude, and each wave decays at a rate determined by its own "τ". Thus, the short wavelength terms die away very rapidly and the homogenization will ultimately be determined by τ for the longest wavelength component.

* Calculation of the wavelength (λ) of the composition fluctuations

→ **Free Energy change for the decomposition**

1) Decomposition of X_0 into $X_0 + \Delta X$ and $X_0 - \Delta X$

What would be an additional energy affecting spinodal decomposition?

In practice, it is necessary to consider two important factors

2) interfacial energy

3) coherency strain energy

1) Decomposition of X_0 into $X_0 + \Delta X$ and $X_0 - \Delta X$

$$\Delta G_{chem} = \frac{1}{2}\frac{d^2G}{dX^2}(\Delta X)^2$$

Gibb's free energy reduction by compositional change

$$f(a+h) = f(a) + f'(a)h + \frac{f''(a)}{2!}h^2 + \cdots$$

$$G(X_0 + \Delta X) \approx G(X_0) + G'(X_0)\Delta X + \frac{G''(X_0)}{2!}\Delta X^2$$

$$G(X_0 - \Delta X) \approx G(X_0) - G'(X_0)\Delta X + \frac{G''(X_0)}{2!}\Delta X^2$$

$$\Delta G_{chem} = \frac{G(X_0 + \Delta X) + G(X_0 - \Delta X)}{2} - G(X_0)$$

$$= \frac{G''(X_0)}{2!}\Delta X^2 = \frac{1}{2}\frac{d^2G}{dX^2}\Delta X^2$$

5.5.5 Spinodal Decomposition

2) During the early stages, the interface between A-rich and B-rich region is not sharp but very diffuse. → diffuse interface

ΔG by formation of interface btw decomposed phases

Interfacial Energy
(gradient energy)

∝ composition gradient across the interface
: increased # of unlike nearest neighbors in a solution containing composition gradients

$$\Delta G_\gamma = K\left(\frac{\Delta X}{\lambda}\right)^2$$

Max. compositional gradient ΔX/λ

K : a proportionality constant dependent on the difference in the bond energies of like and unlike atom pair

If the size of the atoms making up the solid solution are different, the generation of composition differences, ΔX will introduce a coherency strain energy term, ΔGs.

3) Coherency Strain Energy
(atomic size difference)

$$\Delta G_S \propto E\delta^2 \Leftarrow \delta = (da/dX)\,\Delta X/a$$

δ: misfit between the A-rich & B-rich regions, E: Young's modulus, a: lattice parameter

$$\Delta G_S = \eta^2(\Delta X)^2 E' V_m$$

$$\text{where } \eta = \frac{1}{a}\left(\frac{da}{dX}\right), E' = E/(1-\nu)$$

ΔGs~ independent of λ

η: the fractional change in lattice parameter per unit composition change

* Total free E change by the formation of a composition fluctuation
1) + 2) + 3)

$$\Delta G = \left\{\frac{d^2G}{dX^2} + \frac{2K}{\lambda^2} + 2\eta^2 E' V_m\right\}\frac{(\Delta X)^2}{2}$$

5.5.5 Spinodal Decomposition

* Total free E change by the formation of a composition fluctuation

$$\Delta G = \left\{ \boxed{\frac{d^2G}{dX^2} + \frac{2K}{\lambda^2} + 2\eta^2 E' V_m} \right\} \frac{(\Delta X)^2}{2}$$

< 0

a) Condition for Spinodal Decomposition

(→ a homogeneous solid solution~unstable)

$$-\frac{d^2G}{dX^2} > \frac{2K}{\lambda^2} + 2\eta^2 E' V_m$$

b) The Limit of T and composition in coherent spinodal decomposition

(스피노달 분해가 일어나는 온도와 조성의 한계값)

$$\lambda \rightarrow \infty$$

$$\frac{d^2G}{dX^2} = -2\eta^2 E' V_m$$

→ **coherent spinodal**

It lies entirely within the chemical spinodal ($d^2G/dX^2=0$)

(boundary btw ③ & ④, next page)

Wavelength for coherent spinodal

$$\lambda^2 > -2K \Big/ \left(\frac{d^2G}{dX^2} + 2\eta^2 E' V_m \right)$$

→ The minimum possible wavelength (λ) decreases with increasing undercooling (ΔT~ΔX) below the coherent spinodal.

This figure include the lines defining the equilibrium compositions of the coherent/ incoherent phases that result from spinodal decomposition.

* Incoherent(or equilibrium) miscibility gap: $\Delta H > 0$

The miscibility gap the normally appears on an equilibrium phase is the incoherent (or equilibrium) miscibility gap.→ equilibrium compositions of incoherent phases without strain fields.

a) chemical spinodal: $d^2G/dX^2=0$_no practical importance X

b) Area ② , $\Delta G_V - \Delta G_S < 0$ → only incoherent strain-free nuclei can form.

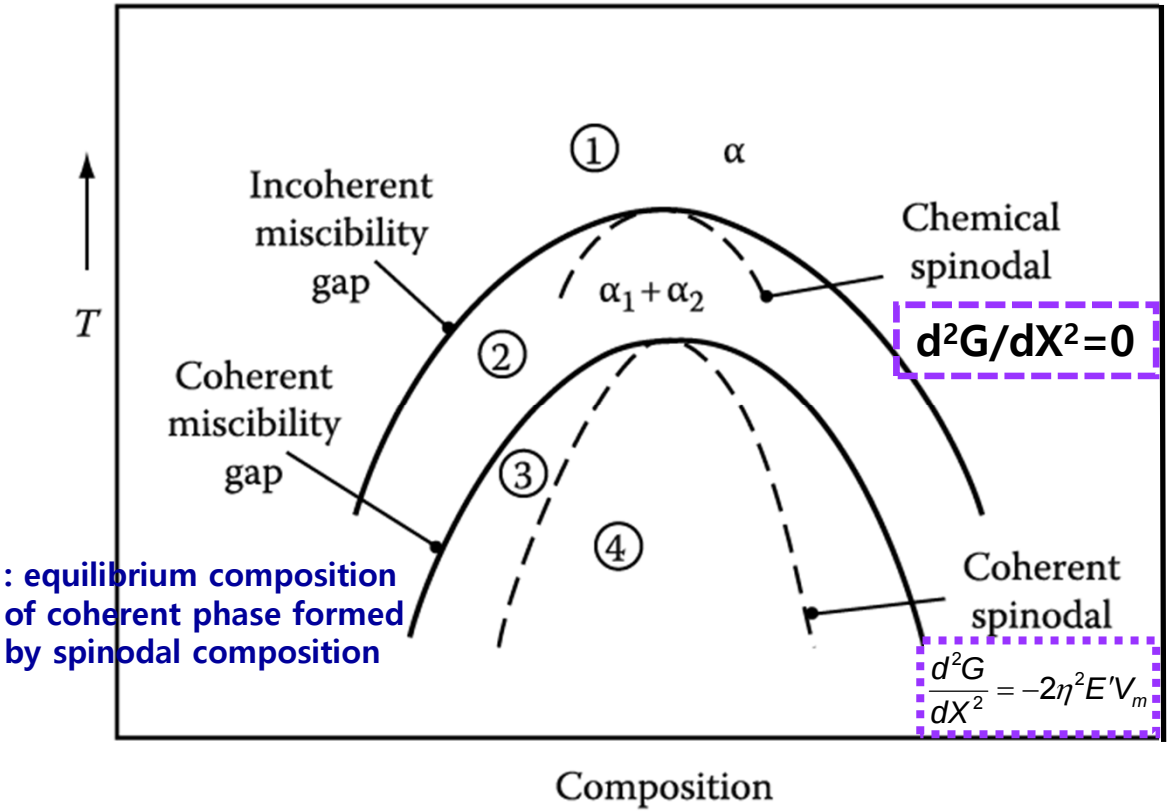

Figure 5.41 Schematic phase diagram for a clustering system.

Region 1: homogeneous α stable. Region 2: homogeneous α metastable, only incoherent phases can nucleate. Region 3: homogeneous α metastable, coherent phase can nucleate. Region 4: homogeneous α unstable, no nucleation barrier, spinodal decomposition occurs.

Spinodal decomposition is not only limited to systems containing a stable miscibility gap

All systems in which *GP zones* form, for example, containing a metastable coherent miscibility gap, i.e., the GP zone solvus.

→ at high supersaturation, GP zone can form by the spinodal mechanism.

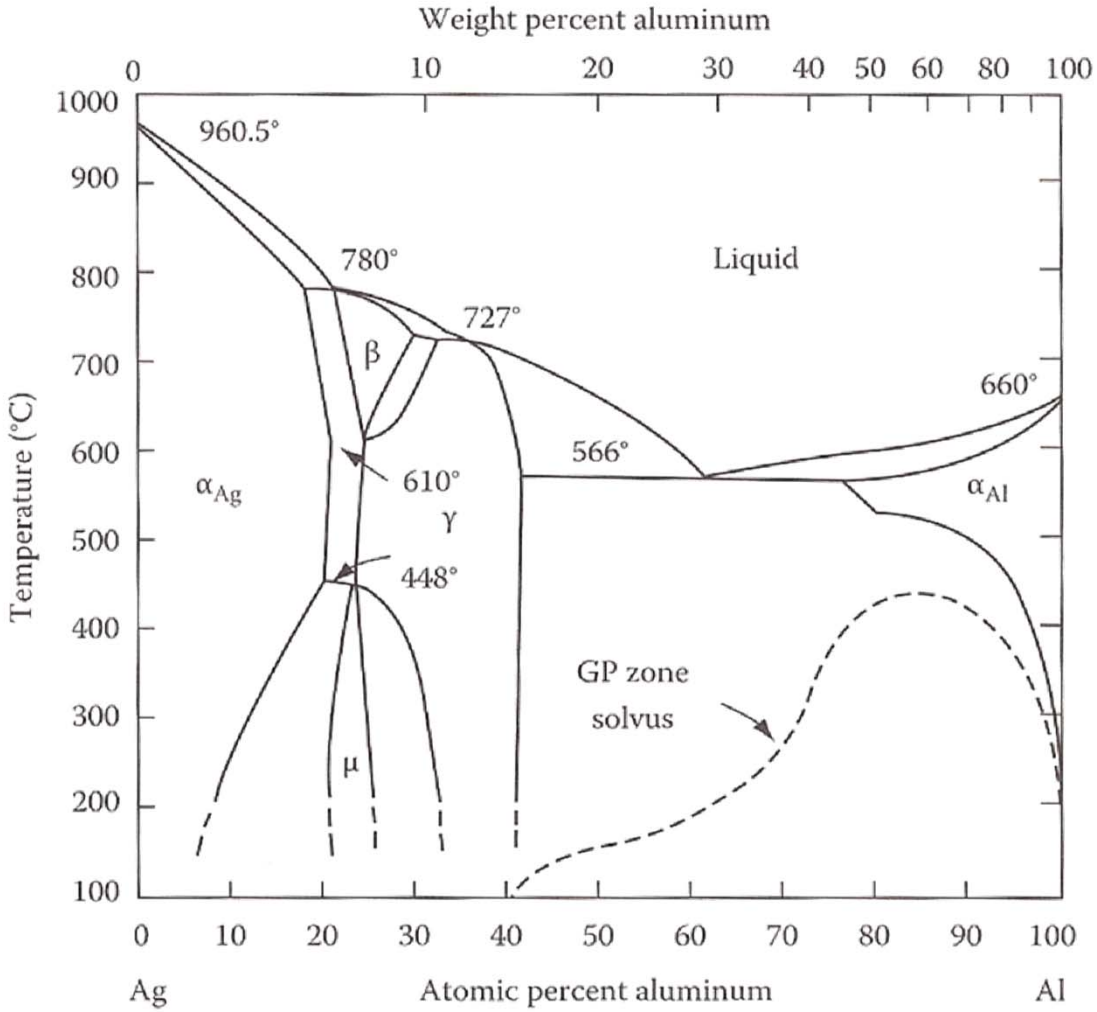

Figure 5.34

Al-Ag phase diagram showing metastable two-phase field corresponding to GP zones.

- The difference in T between the coherent and incoherent miscibility gaps, or the chemical and coherent spinodals ∝ **magnitude of** $|\eta|$ η: the fractional change in lattice parameter per unit composition change
- Large atomic size difference → $|\eta|$ **large**→large undercooling to overcome the strain E effects
- Like Al-Cu, large values of $|\eta|$ in cubic metals can be mitigated if the misfit strains are accommodated in the elastically soft <100> directions. → composition modulations building up normal to {100}

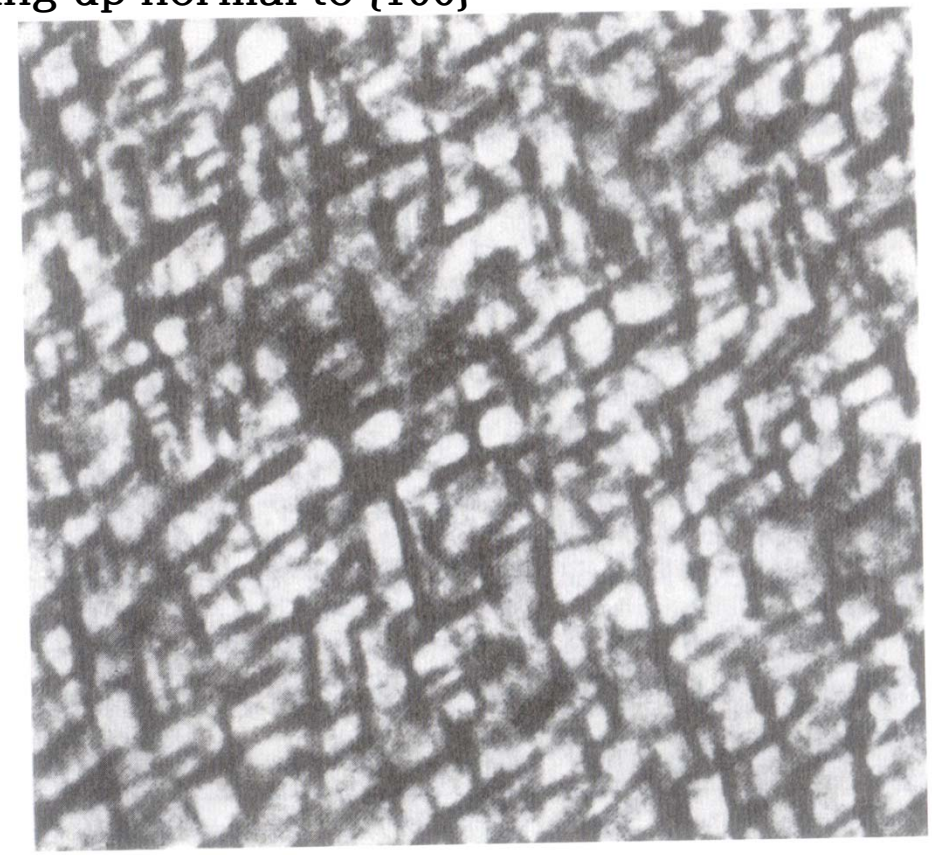

Figure 5.42 A coarsened spinodal microstructure in Al-22.5 Zn-0.1 Mg (at%) solution treated 2h at 400 ℃ and aged 20h at 100℃. Thin foil electron micrograph. λ = 25 nm_coarsening

Contents for today's class

- **Precipitation in Age-Hardening Alloys**

α_0 Quenching + Isothermal

$\rightarrow \alpha_1$+GP zones

$\rightarrow \alpha_2+\theta'' \rightarrow \alpha_3+\theta' \rightarrow \alpha_4+\theta$

Transition phases

GP Zones → $\alpha_2+\theta''$ → $\alpha_3+\theta'$ → $\alpha_4+\theta$ ($CuAl_2$)

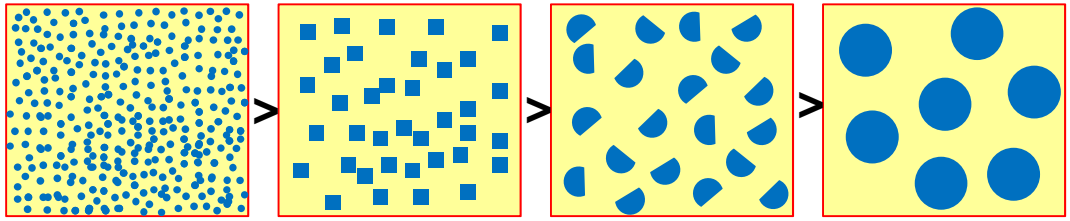

All coherent partially coherent Incoherent

Maximum hardness~ largest fraction of θ″
(coherent precipitates)

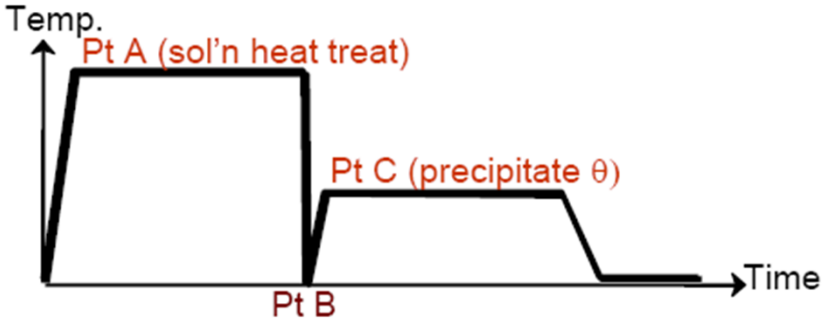

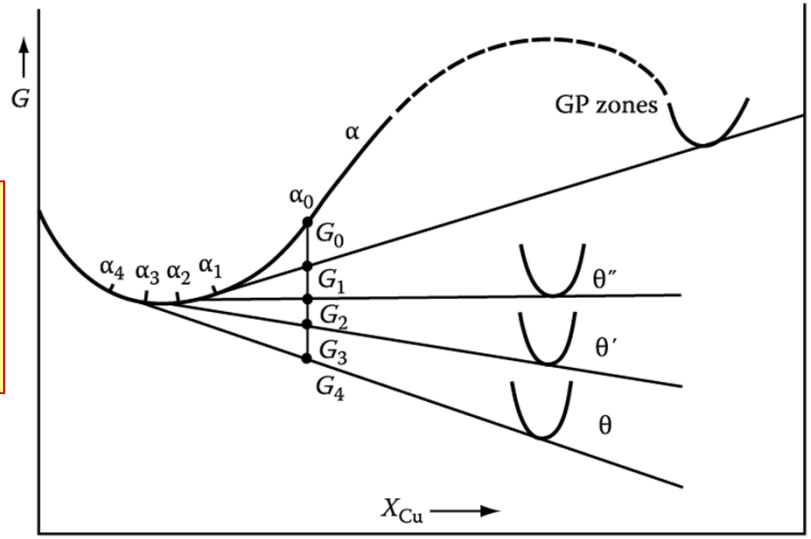

- **Quenched-in Vacancies**

If $X_v < X_v^c$ critical vacancy supersaturation,
Precipitate nucleation X → formation of PFZ

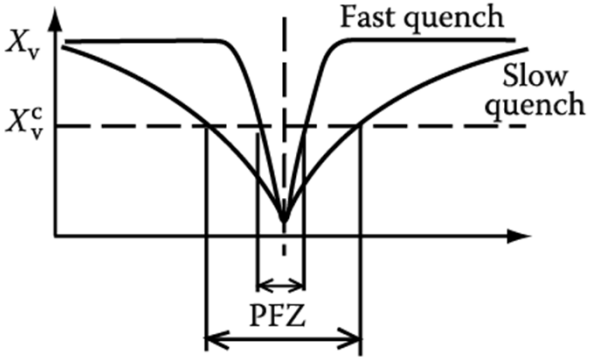

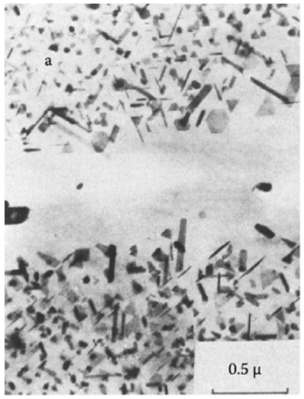

5.5.4. Age Hardening

Transition phase precipitation → great improvement in the mechanical properties

Coherent precipitates→highly strained matrix→the main resistance to the Ⓓ movement: solid solution hardening

Hardness vs. Time by Ageing

Maximum hardness~ largest fraction of θ″
(coherent precipitates)

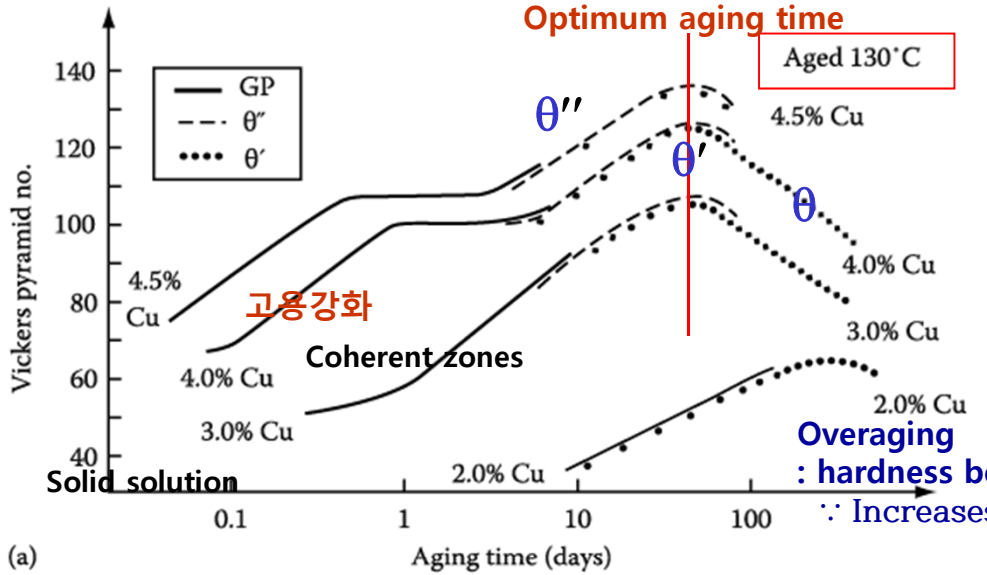

Ageing at 130°C produces higher maximum hardness than ageing at 190°C.

At 130°C, however, it takes too a long time (several tens of days).

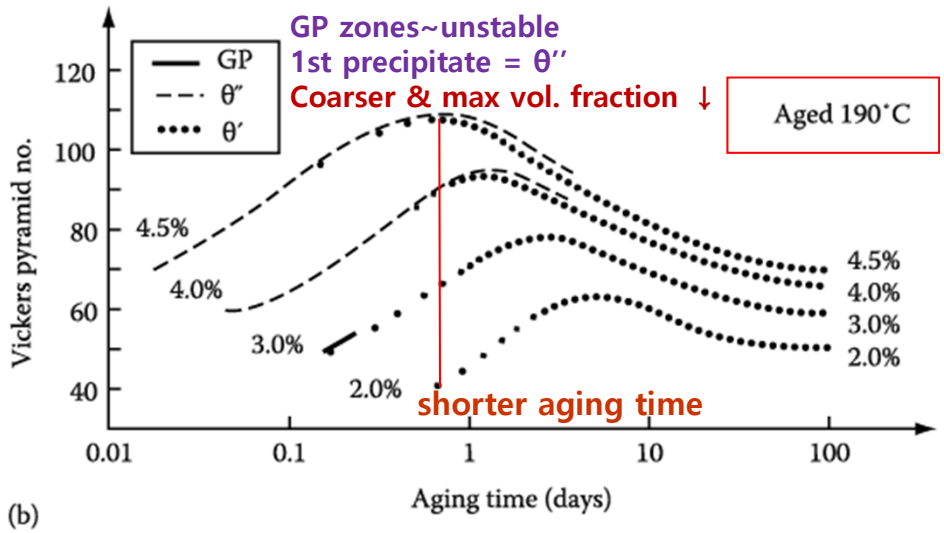

How can you get the high hardness for the relatively short ageing time (up to 24h)?

Double ageing treatment

first below the GP zone solvus → fine dispersion of GP zones then ageing at higher T.

: Engineering alloys are not heat treated for max. strength alone. → **to optimize other properties**
best heat treatment in practice

Fig. 5. 37 Hardness vs. time for various Al-Cu alloys at (a) 130 ℃ (b) 190 ℃

• Spinodal Decomposition

Spinodal mode of transformation has no barrier to nucleation

: describing the transformation of a system of two or more components in a metastable phase into two stable phases

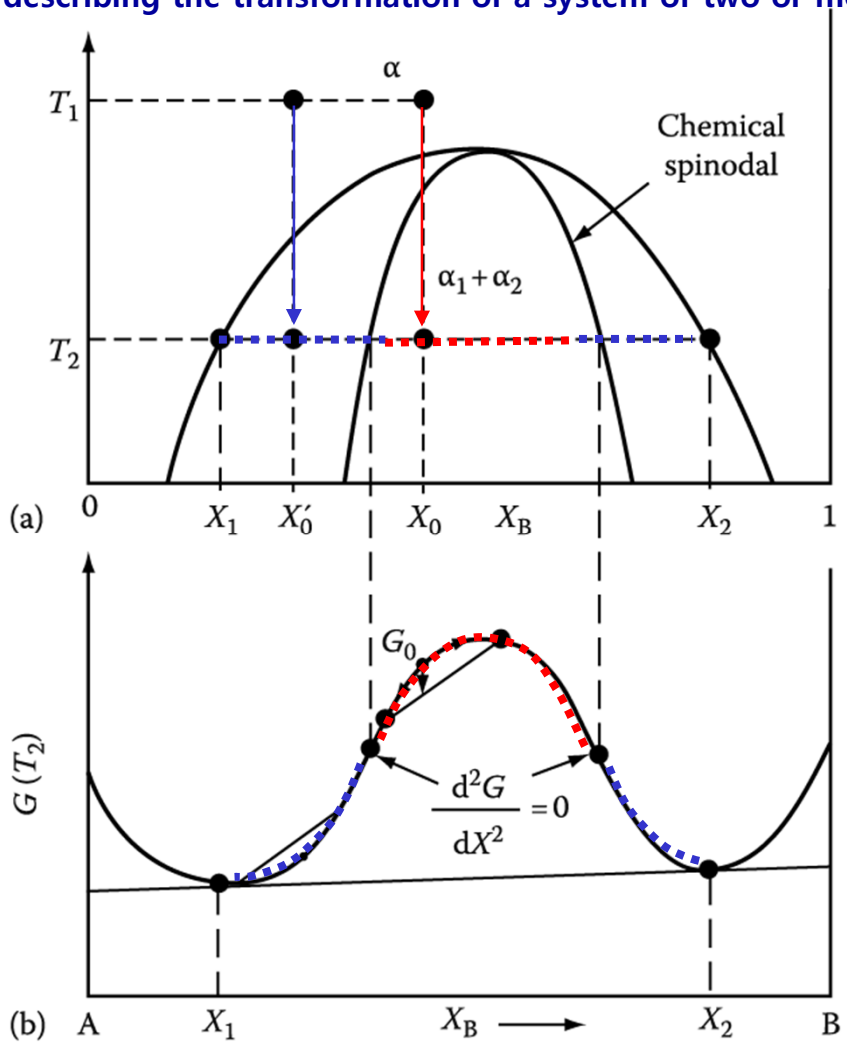

Fig. 5.38 Alloys between the spinodal points are unstable and can decompose into two coherent phasees α_1 and α_2 without overcoming an activation energy barrier. Alloys between the coherent miscibility gaps and the spinodal are metastable and can decompose only after nucleation of the other phase.

How does it differ between inside and outside the inflection point of Gibbs free energy curve?

1) Within the spinodal $\frac{d^2G}{dX^2}<0$

: phase separation by small fluctuations in composition/ "up-hill diffusion"

2) If the alloy lies outside the spinodal, small variation in composition leads to an increase in free energy and the alloy is therefore metastable.

The free energy can only be decreased if nuclei are formed with a composition very different from the matrix.

→ nucleation and growth

: "down-hill diffusion"

This figure include the lines defining the equilibrium compositions of the coherent/ incoherent phases that result from spinodal decomposition.

* Incoherent(or equilibrium) miscibility gap: $\Delta H > 0$

The miscibility gap the normally appears on an equilibrium phase is the incoherent (or equilibrium) miscibility gap.→ equilibrium compositions of incoherent phases without strain fields.

a) chemical spinodal: $d^2G/dX^2=0$_no practical importance X

b) Area ② , $\Delta G_V - \Delta G_S < 0$ → only incoherent strain-free nuclei can form.

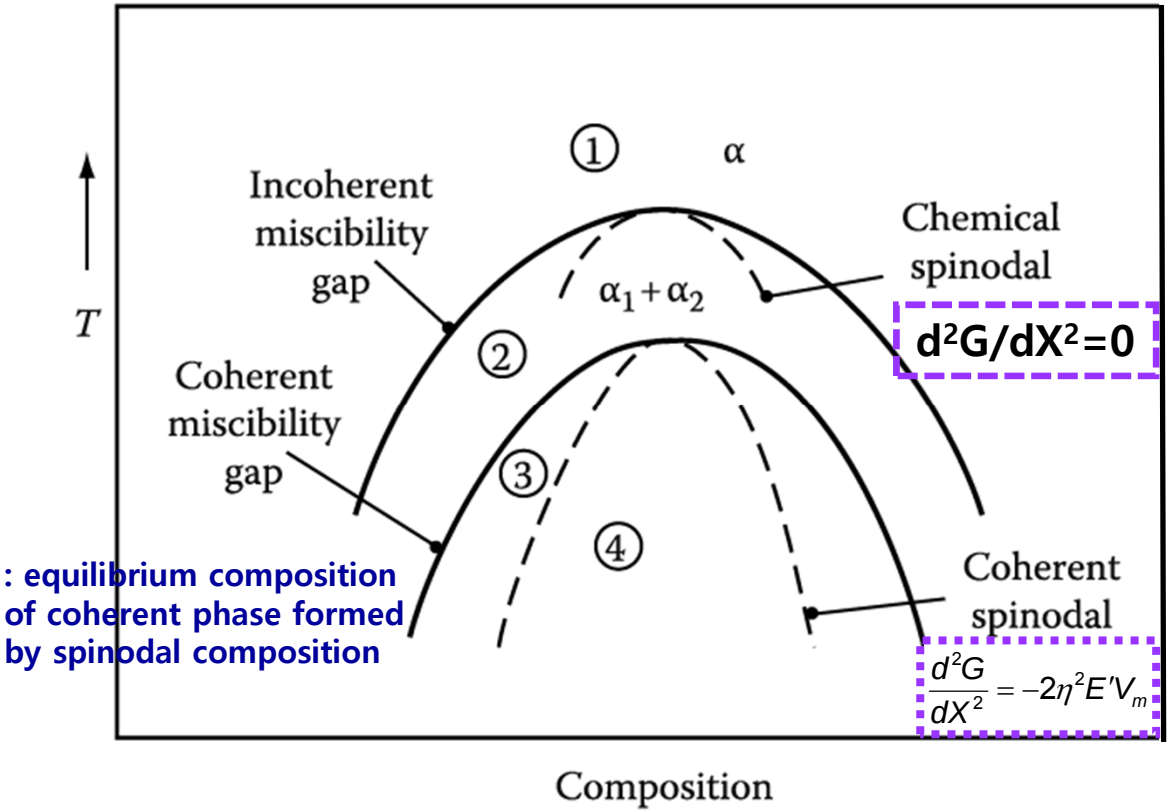

Figure 5.41 Schematic phase diagram for a clustering system.

Region 1: homogeneous α stable. Region 2: homogeneous α metastable, only incoherent phases can nucleate. Region 3: homogeneous α metastable, coherent phase can nucleate. Region 4: homogeneous α unstable, no nucleation barrier, spinodal decomposition occurs.